Thermal Design and Analysis of Static Chamber Microfluidic Device

Author

Mohsin Raza

Registration Number

00000119573

Supervisor

Dr. Imran Akhtar

Co-Supervisor

Dr. Imran Raouf Malik

DEPARTMENT OF MECHANICAL ENGINEERING

COLLEGE OF ELECTRICAL & MECHANICAL ENGINEERING

NATIONAL UNIVERSITY OF SCIENCES AND TECHNOLOGY

ISLAMABAD

August, 2019

Thermal Design and Analysis of Static Chamber Microfluidic Device

Author

Mohsin Raza

Registration Number

00000119573

A thesis submitted in partial fulfillment of the requirements for the degree of

MS Mechanical Engineering

Thesis Supervisor:

Dr. Imran Akhtar

Thesis Supervisor's Signature: _____

DEPARTMENT OF MECHANICAL ENGINEERING

COLLEGE OF ELECTRICAL & MECHANICAL ENGINEERING

NATIONAL UNIVERSITY OF SCIENCES AND TECHNOLOGY,

ISLAMABAD

August, 2019

Declaration

I certify that this research work titled "***Thermal Design and Analysis of Static Chamber Microfluidic Device****"* is my own work. The work has not been presented elsewhere for assessment. The material that has been used from other sources it has been properly acknowledged / referred.

Signature of Student: _____

Mohsin Raza

Registration Number: 00000119573

Language Correctness Certificate

This thesis has been read by an English expert and is free of typing, syntax, semantic, grammatical and spelling mistakes. Thesis is also according to the format given by the university.

Signature of Student: _____

Mohsin Raza

Registration Number: 00000119573

Signature of Supervisor: _____

Dr. Imran Akhtar

Plagiarism Certificate (Turnitin Report)

This thesis has been checked for Plagiarism in Turnitin .The report countersigned by respective supervisor is attached along with.

Signature of Student: _____

Mohsin Raza

Registration Number: 00000119573

Signature of Supervisor: _____

Dr. Imran Akhtar

Copyright Statement

Acknowledgements

I would like to thank everyone who has supported me since I began my graduate studies here at NUST. Your love, support and encouragement has made my experience here much more enjoyable and rewarding. Sometimes nothing seems to go in the right direction; you need to have patience and persistence, which would not have been possible without the support of my friends, family and loved ones.

First and foremost, I would also like to express special thanks to my supervisor Dr. Imran Akhtar for his help throughout my thesis. I admire his passion and dedication to his research and students. Dr. Imran Raouf Malik was the first person who introduced me to the field of microfluidics. He got me started on this PCR Device design project and pushed me to tackle some interesting problems. I would also like to pay special thanks to Dr. Zafar Abbas Bangash for their support and service on my committee. I need to thanks my friends, Ali Raza, Muteeb ul Haq, Ali Javaid and Amir Hiraj for his kind suggestions and the discussions we had on different topics.

Finally, I thank my parents and brothers for their care and love. Your support and encouragement has been the backbone of my life. Thank you for always believing in me.

Dedicated to my Parents and adored siblings whose tremendous support and cooperation led me to this wonderful accomplishment

Abstract

Infectious diseases constitute a major cause of disease burden and more than half a billion Disability -Adjusted Life Year's (DALYs) and millions of deaths each year. They have large effect on children under 5 years of age especially. To provide the healthy life to people the disease diagnostic are very essential on early stages so that an early cure can control the disease.

For the purpose of drug discovery, Infectious disease diagnostics, on site evidence collection system pathology and food science, the Polymerase chain reaction (PCR) method is used. Polymerase chain response (PCR) can make duplicates of specific parts of DNA by thermal cycling. An average three-step PCR incorporates denaturation of double stranded DNA (92–98 °C), the primers annealing (50–60 °C), and extension of single strand DNA to double strand DNA (68–72 °C). Each thermal cycle can double the quantity of DNA, and 20–35 cycles can create a large number of DNA copies. The continuous flow microfluidic device are not suitable for commercial purpose. The static chamber device available in market for 30 microliter sample size, these devices are much expensive. In this study we designed a Well type Sample block for the sample volume of 50 microliter. The Sample block is in rectangular shape 48 (6 by 8) wells with each 50 microliter capacity. The sample block material is aluminum, tubes are made of polypropylene and tube cap made with transparent glass. Initially the cyclic temperature boundary condition is applied and for final analysis thermoelectric component is placed at the base of sample block. The ATE1-TC-70-15AS is number of thermoelectric module, which consisted at 70 cells. Other information can be obtained about Peltier from Analog technologies catalog.

The device results are compared with CFX Bio-Rad design and current study shows the better temperature response rate, temperature uniformity with in fluid sample. The sample block can be made only by machining process. Hence, the proposed scheme paves the way for low-cost point-of-care diagnostics, system integration and device miniaturization, realizing a portable microfluidic device applicable for on-site and direct field uses.

Keywords: Thermal cycling, Microfluidic design, DNA amplification, CFX Bio-Rad, Polymerase chain reaction (PCR), thermoelectric module.

Table of Contents

List of Figures

List of Tables

CHAPTER 1

INTRODUCTION

1.1. Overview

In this section we will establish the importance of POC (point of care) diagnostics in healthcare and the merits of PCR based pathogen and biomarker detection. First, we will provide an overview of the burden of disease in the world and then we will show the expected impact opportunity of diagnostic technologies, especially focusing on the comparison between developing world and low income regions. 'Appropriate' diagnostics technologies have the potential to revolutionize healthcare in developing world immediately and in developed world eventually especially for infectious diseases. Molecular diagnostics (MDx) is also becoming very important in diagnostics and cure of communicable diseases such as cancer and cardiovascular disease. Everybody in the world will eventually die and nothing in the world can prevent this. It is estimated that 107 Billion have ever lived on Earth i.e., about 15 dead people for each living person at the present time. However, the cause of death varies among humans. [1]

The average lifespans also varies in different regions, and the prevalence of disease varies widely as do the average income levels. Most of these deaths are due to diseases of various kinds. Clearly, the impact of disease on human population is large, and while everyone will eventually die, diseases clearly lead to lower quality of life and productivity. To increase the quality of life there need to make devices which can use to identify the diseases as cheap as possible. For the diagnostics of diseases different type of test required, the microfluidic is field of engineering in which design the devices for lowest sample size.

Microfluidic systems are a subject of interest since past few decades because of short time of reaction and a pretty fast transition during the process. Microfluidic chips found many applications in the field of biomedical engineering and in the fields of genetics. In 1986 when PCR (polymerase chain reaction) was invented [2], microfluidic systems became an important regime that found its application on the micro scale biochemical reactions. Polymerase chain reaction (PCR) is a biochemical process for an in-vitro enzymatic amplification of nucleic acid. The objective of PCR

is to amplify a single template to produce the copies by square power for each cycle. PCR finds its wide applications in the field of clinical sciences, medical diagnostic, biological drug discovery and also in genetic analysis.

Generally there two comprehensive ways in which we can perform the microfluidic thermo cycling. These are continuous flow PCR and static chamber PCR. The working principle of static chamber PCR devices is almost same as of conventional thermocyclers. The sample is the static chamber device is static and both sample and the device undergo the thermal cycling operations [3-5]. In static chamber PCR devices thermal cycling is attained by the natural convection due to the temperature gradients present between the two thermal plates that are kept above the denaturation and below the annealing temperatures [6-7]. Thermal inertia in the early continues devices was high as compared to the static chamber PCR devices. At the time the power of pump is also required to flow the sample through micro channels and it's not efficient way to amplify the DNA. At a time only one sample can be tested in continues devices but in static chamber can be placed more than one sample, which reduce the overall testing cost of samples. SC devices require the high consumption of energy due to the thermal inertia and cycling process got longer [8-10] but when used more than one samples at a time, the required energy is less as continues system. To achieve the rapid heating and cooling rate to reduce the thermal mass of static chamber different changes were made e.g. Aluminum alloy was used to manufacture the microfluidic PCR sample block [11-12]. The computational study couples the mass conservation of species and PCR kinetics with the heat transfer, Peltier heating and temperature controller. In the static chamber devices most common approaches are the solution of heat transfer equations [13-14]. Some studies couple the controller function with the static chamber devices [15].

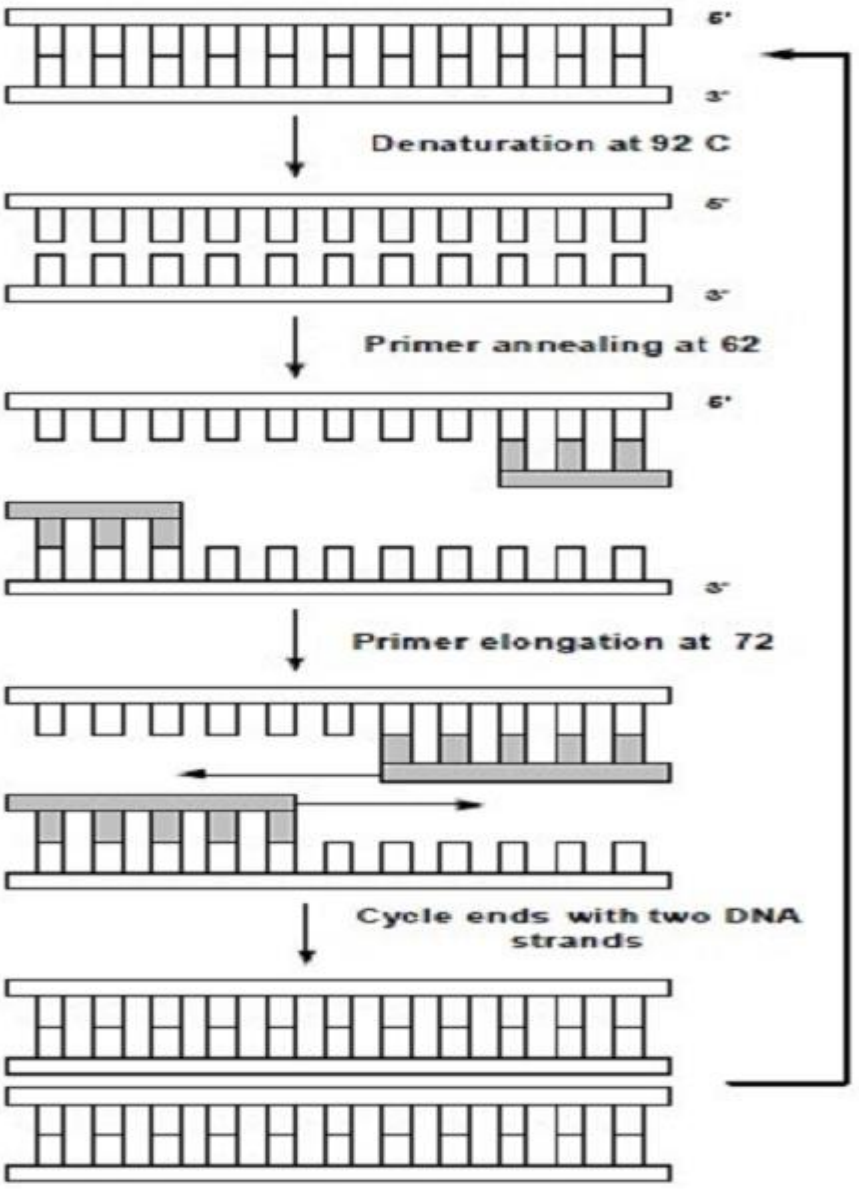

Figure 1.1: Amplification process of PCR involving three temperature zones [16].

1.2. Fundamental Components of PCR system

PCR process consists of five main components that are necessary to perform the PCR process. These five key components are briefly summarized here.

i. First one is the DNA template that is a target which has to be copied.

ii. There are short pieces of DNA which are called primers, whose function is to match the DNA template.

iii. Nucleotides of DNA that also known as triphosphates are made of four types of bases (A, C, G and T) which works as building blocks of DNA. In the process of PCR these triphosphates are necessary to make the new strands of DNA.

iv. DNA polymerase are complex are complex proteins which are used to build the new strands of DNA by using primers and triphosphates.

v. Buffers are used to provide the suitable environment for the reaction.

1.3. Applications of PCR

PCR finds its various applications in the different fields including the clinical sciences, genetic analysis and medical diagnosis. Some important applications of PCR are given below.

i. PCR finds it enormous applications in the detection of various viral health diseases such as AIDS, tuberculosis and influenza virus.

ii. Sometimes genetic problems occur due to innate changes or natural mutations. PCR helps in the diagnosis of these types of genetic diseases.

iii. PCR is used in the identification of fingerprints for different purposes.

iv. PCR is used to trace the evolutionary and cultural lineage of living beings.

v. PCR is used extensively for microbial surveillance of the environment.

vi. Detection of pathogens in food, water and in tissue specimens is done through the PCR.

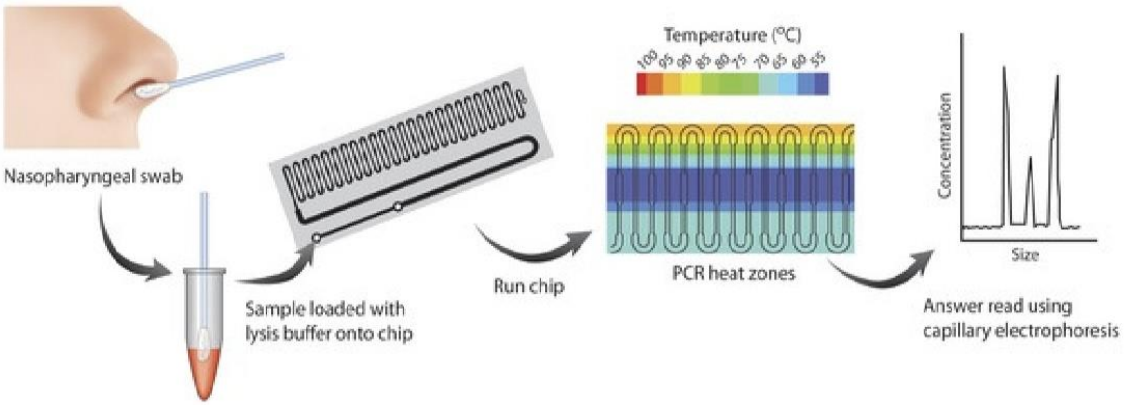

Figure 1.2: PCR infectious disease diagnosis.

1.4. Motivations

Micro electromechanical (MEMS) have become very advanced in the current age and its growth has shown a pretty fast advancement. The worth of MEMS industry was $6 billion in the 2006 and this grown up to $11.9 billion that is a handsome increment. This growth was more than the expected growth according to the experts in this industry. In this sector microfluidic devices and bio MEMS are a big contributor with the worth of $2.7 and $2.56 billion in the fiscal year of 2015 respectively. This constant growth in the industry of MEMS and microfluidic devices is a source of motivation to develop the PCR devices to share the market worth. PCR devices are being used worldwide to diagnose the serious health diseases and their treatment e.g. cancer and other blood related diseases in the medical laboratories. Currently in Pakistan growth rate of cancer is being increased at an alarming level and 12 deaths are occurring in 100 reported cases. This issue can be overcome by growing the local MEMS industry to provide the cheap equipment that is used in to the biomedical and pathology laboratories. In this way a handsome reduction in cost can be observed. Restriction Fragment Length Polymorphism (RFLP) is an old method to perform some specified DNA relates tests. In this technique amount of DNA required is large and also it must be graded. When conditions become hot or moist then degradation of DNA occurs at high rates and in these conditions RFLP method fails to give the required results. PCR is a technique that has replaced this method in the current forensic science and medical laboratories. The present research work is motivated from the above mentioned data and considerations for the local industrial growth to produce a feasible static chamber thermoelectric PCR device. In the developing countries many infectious diseases are causing the disability and burden of deaths in the people. If an access can be granted to the proper treatment of these infectious diseases in a cheaper way then death rate can be decreased in an appreciable manner. In some cases there is no need to conduct the test for the diagnosis of disease or infection but in some cases it is necessary to perform some specific pathological test for accurate diagnosis. In many developing countries proper diagnosis test are not available so they rely on the technique of point of care (POC). Lack of rules and regulations in many developing countries cases the poor POC tests which finally results in the poor diagnosis. In the current scenario PCR devices are of a great importance for these countries that can perform the test for many fatal diseases in an accurate way with a very reasonable investment. Many medical centers in the developing countries just rely on the physical clinical judgment that cannot be an accurate diagnosis for some fatal bacterial diseases. So, if

cheaper PCR devices are available to those hospitals where a common person needs the proper diagnosis and treatment of his disease then life would be much easy rather than involving the wrong clinical analysis.

1.5. Contributions

Conventional CF-PCR have different limitations in terms of their design, cost, and sizes. These are important factors and need consideration in manufacturing the PCR devices. One important factor is the PCR device is the heating process. In the present work heating processes are analyzed by applying a 3D convective heat transfer model for static chamber PCR calculations. There are different parameters in the SC-PCR device that affects the efficiency and performance of the device. To determine which one affects the most a parametric study is performed. Some parameters are critical to design a low mass rapid response PCR sample block and some are not. Critical parameters are listed in a way to specify their affects. The major contribution of this work is to develop a SC-PCR device for DNA amplification. Different kinetic parameters are developed in the formulation of current PCR kinetic model to evaluate the DNA amplification performance.

1.6. Thesis Outline

The detail of chapters are given below, which topics discussed.

Chapter 1 presents the overview of PCR, its fundamental component, applications and importance PCR devices for infectious daises. In chapter 2, detail literature review about available device methods of heating and cooling and technologies in PCR devices presented. The design detail of parts involved in PCR device is discussed in Chapter 3. Chapter 4 presents FEM based 3-dimensional heat transfer mathematical model, PCR kinematics modeling and Peltier heat transfer model. The simulation setup validation and comparison of results of current study and Bio-Rad CFX [1] presented in chapter 5. In chapter 6, the numerical results of sample block results and thermoelectric modules basic results. Finally, the conclusions and future work that can be further performed from this research is also presented in chapter 6. And some drawings of sample block given at end. The objective of this thesis is design a sample block with lowest mass and rapid response of temperature change for the sample size of 50 microliter.

CHAPTER 2

LITERATURE REVIEW OF PCR DEVICES

2.1. Introduction

Kari Mullis invented the polymerase chain reaction (PCR) 30 years ago, since then it has gain great importance in the field of molecular biology as it allows exponentially amplification of deoxyribonucleic acid (DNA) [18]. With only a few PCR cycles, millions of copies can be generated of DNA using only a single molecule. A PCR cycle consists of three basic steps, denaturation, annealing and extension. In the denaturation stage (~ 95 ° C), the DNA with double strands also called denaturants are converted into two single chains. Thereafter, the temperature is reduced prior to the annealing (~ 56 ° C). The primers, which are short complementary DNA sequences, can be attached to the single strand target DNA.

Polymerase are mostly derived from thermophilic organisms like the Thermos aquatics [19]. In order to enhance the Polymerase activity, the temperature of the extension step increases, up to 72 ° C. Activity is received by polymerase for making a second DNA complementary strand using the nucleotides synthesized from solution. This is the reason that the concentration of double-stranded DNA rises exponential by repeating three stages for temperature. This procedure has also been applied to the PCRs having reverse transcription [20].

For a ribonucleic acid (RNA) molecule, a transcription step are carried out in reversed direction for obtaining the DNA complementary to RNA chain prior to PCR. PCR are modified further by introducing fluorescent dyes into the mixture, which helps us to monitor the real progress with [21]. DNA copies are obtained from reaction mixture of extension method using standard curves. This method is known as real-time quantitative PCR (qrt-PCR). Now a days PCR is being used in several fields like, Diagnosis and medicine, agricultural sciences, and food science [22-25]. There are some influential properties associated with the microfluidic devoices that includes the low thermal inertia, fast heat transfer rates and low thermal mass. These properties present in the microfluidic devices are advantageous many ways as compared to the macroscopic devices. Operations in the system become economical due to reagent consumption and reduction in sample

by virtue of small volumes. But volumes in many cases are yet large for the application of bulk kinetics. Additionally different functions can also be integrated in these microfluidic devices easily [26]. Mass transport due to diffusion and heat conduction change with the characteristic length of the system. But in the macroscopic systems above mentioned processes are slow for efficient transport of mass. Convective heat and mass transport are difficult to control in macroscopic devices. Heat conduction and mass diffusion effects are easier to control in the microfluidic devices. Hence processes are controlled in a better way in the microfluidic devices as compared to the macroscopic. High surface to volume ration can be achieved by reducing the size of device. In this way a large area is available for heat and mass transfer. PCR devices involve many cooling and heating processes and time required for analysis can be reduced greatly by miniaturization [27, 28]. Very first flow through PCR was shown by Kopp et.al [29] in 1998. In a microfluidic channel a sample was flown repeatedly and there were three different zones of temperature for PCR. A sample of 10 ml performed 20 cycles of PCR in the span of 90 seconds. A number of applications of PCR in the microfluidic devices are described in the [30, 31]. Because of the low sample and power consumption these PCR devices are of great for point of care applications. If the sample preparation process for PCR and the process of detection is performed in a same microfluidic device. It will reduce the handling time and will prevent the possibility of sample contamination. This research discusses several designs of PCR in microfluidic device from past few years, First of all the basic PCR microfluidic devices are introduced and then their counterpart like time domain PCR microfluidic devices, these are followed by the , (Table 1) shows the amplification of isothermal nucleic acid and digital PCR in microfluidic devices .

2.2. Space Domain PCR

If the sample moves in a micro channel at various temperatures corresponding to its length, the temperature will depend on the position it has acquired with in the channel. Therefore, these devices are known as space domain PCR device. Preparation of the sample can be easily incorporated into the microfluidic device. Duration for the PCR thermal steps and the number of cycles are dictated by the design of microfluidic. The working of the PCR devices depends on the sample movement along the channel.

Table 2.1: Varies type of PCR devices in literature

Method	Design & System	Approach	Ref.
Space domain	Serpentine channel designs	Disposable polyimide chip 30 cycles of PCR	34
		CNC fabricated polycarbonate device 30 cycles of PCR	35
		Steel capillary coated with NOA61 Reducing back pressure	36
		Metal–polymer composite material Improved temperature stability	37
		Replacing active pumps with capillary forces Model of capillary forces in channel for PCR	38
		Reducing the number of heaters Central heater, edges of chip cooled by heat pipes	39
		Reducing the number of heaters 3D device heated at the bottom	40
	Radial designs	Radial design Central heater, edges actively cooled	41
		Radial design Heated by focusing sunlight on center of device	42, 43
		Capillary wrapped around cylinder Cylinder with different temperature zones	44
		Centrifugal microfluidic device Mounted on dual shaft centrifuge	45
	Digital and oscillating Designs	Oscillating droplet Four parallel channels for multiplexing	46
		Oscillating droplet Nested PCR to increase specificity	47
		Digital microfluidic device Droplet moved between temperature zones	48
		Digital microfluidic device	49
		Digital microfluidic device	50
	Heating/cooling systems	Capillaries in water bath Forced convection inside capillaries	51
		Sample moved between water baths using servo motor	52, 53
Time domain PCR	Heating/cooling systems	Infrared heating through tungsten lamp Fan for active cooling	54, 55
		Infrared laser for heating	56
		Silicon heating chip Portable real-time PCR device	57, 58
		Silicon heating chip Melting curve analysis, multiplexing	59
		Sample chamber on top of heat exchanger Heating and cooling through medium	60, 61

Method	Design & System	Approach	Ref.
		Silica capillaries with thin film heaters Cooling by fan	62
		Capillary with bypass channel Heating and cooling by Peltier elements	63
	Integrated devices	Lysis and PCR in same chamber	64
		Removal of inhibitors through diffusion Chemical lysis followed by DNA extraction with magnetic particles	65
		Retention of DNA on silica gel membrane Release by master mix and amplification	66
		FTA membrane at entrance of amplification chamber retaining DNA	67
		Dielectrophoresis to capture pathogens on slip chip Followed by washing and PCR	68
		Separation of amplicons by CE after PCR	69, 70
		PCR in amplification chamber connected to CE Real-time detection of amplicons	71
	Centrifugal microfluidic designs	Centrifugal device with chambers Counting of bacteria through Poisson distribution	72, 73
		PCR centrifugal device	74, 75
		Ice-valves next to PCR chamber centrifugal device subdividing sample	76, 77
		Positive, negative control, and internal standards lab Disc device with vapor diffusion barrier	78
		Preventing bubble formation in amplification chamber during PCR Lab Disc device including sample preparation	79
	Arrays	Printed array of sample droplets in oil	80
		Dispensing of single cells onto hydrophilic spots for PCR	81
		Compartmentalization of sample by centrifugal device Detection of amplicons by printed DNA probe array	82
	Single cell devices	Printing of single cells into individual reaction volumes	83
		Trapping of single cells followed by lysis and RNA extraction	84
		Encapsulation of single cells into droplets Droplet sorting to recover genome of target species	85
		PDMS valve to create 96 × 96 array of single cells	86, 87
		300 cell traps separated by valves	88

Method	Design & System	Approach	Ref.
Isothermal Nucleic acid Amplification	Implementation of LAMP on microfluidic devices	Continuous flow LAMP in droplets for DNA and microRNA	89, 90
		Multiplexed LAMP in device with 8 amplification	91
		LAMP in agarose beads	92
		Extraction of RNA using magnetic beads followed by reverse transcription LAMP	93
		Centrifugal device with real-time detection of LAMP reaction	94
		Centrifugal device for multiplexed detection of 10 different species by LAMP	95
		Centrifugal LAMP device including sample preparation and detection of products	96
	LAMP for point-of-care devices	LAMP in capillary heated by two pocket warmers for portable format	97
		Disposable polycarbonate cassette for LAMP	98
		LAMP followed by electrochemical detection	99
		Ten reaction chambers with different primers for multiplexed LAMP, detection by naked eye	100
Digital PCR	Multiplexed digital PCR	Duplexed digital PCR in device containing 38 panels each with 770 partitions	101
		Duplex digital PCR in droplets utilizing TaqMan--probes with different emission wavelength	102, 103
	Various designs	Cross-junction to generate water in oil emulsions for droplet digital PCR	104
		Creating sample array through PDMS membrane	105
		Megapixel digital PCR device	106,107, 108
		Creating droplets at T-junction	109
		Creating sample array with negative pressure vapor proof-layer to stop sample evaporation	110
		Digital PCR in agarose beads	111
		Digital PCR to count nanoparticles tagged with DNA	112
	Integrated systems	Centrifugal device dividing samples into reaction volumes	113
		Centrifugal device using step emulsification for creating droplets	114–116
		Device combining sample preparation and digital PCR	117, 118
		Slip chip for digital PCR	119–120
Commercial PCR devices	Integrated devices	Centrifugal system with sample preparation and detection	121

Method	Design & System	Approach	Ref.
		Automated systems including sample preparation, amplification and detection using prefilled reagent strips or blister-films	122–123
		Integrated, automated systems utilizing cartridges	127, 128
		Microfluidic silicon chip, with hybridization array for detection	124
	Digital PCR devices	Based on an array of chambers	125
		Droplet based	126, 127
		Integrated fluidic circuits for sample portioning	128

2.3. Time Domain PCR

In these devices, the temperature is changed while the samples remain stationary. The temperature of the sample depends on the climate; consequently it is called a time-domain PCR device. Since the temperature profile does not depend on designing of the channel, it is possible to modify the thermal cycle of the PCR by modifying the Heating and cooling procedures of the device. Since sample is stationary, no pumps are required. A drawback of this mode is that the devices cannot be operated continuously by limiting the sample flow.

2.3.1 Various methods for heating and cooling

Various heating and cooling methods. Devices in the time domain depend on an adequate temperature gradient in a stationary sample so in order to insure active heating and cooling of the sample more sophisticated systems are required than most ordinary PCR devices. Various new techniques for rapid cooling and heat control are being considered. A common option for heating is by using infrared light, as it heats the system without the steps of conduction or convection. In one method a tungsten lamp is used for infrared heating and a fan to ensure forced convection for cooling, Rates of heating and cooling obtained using this method are 10 ^{o} C/s [32]. Two distinct lasers with their own unique frequencies were used for the excitation of the two dyes, Eva Green and ROX. Photomultiplier tube (PMT) was used for collecting the emissions that were demodulated by frequency analysis. Pak et al. used an infrared laser at 1450 nm to heat a 1.4 µl sample into a microfluidic chamber [33]. Heating speeds of up to 60 ° C /s could be achieved with a laser instead of a tungsten lamp. The microfluidic devices that are small in size enable fast heating. The photo thermal conversion of Plasmon was employed in one case by exposing a thin layer of gold in the microfluidic chamber for PCR along with the LEDs [34]. If photon-electron-

phonon coupling is performed using the membrane made of hold then the heated solution can be obtained in three minutes at heating rates of 79 ° C /s. In another example, small heated masses are used to place sample droplets (about 200 μl) on a hydrophobic glass and covered with the droplets of small mineral to prevent evaporative silicone device [35] with heating resistors from gold and temperature sensors parallel to four samples to warm up. In combination with the unit for optical detection along with an external power supply of 12 V, the system forms a real-time portable PCR device. Low temperature gradients along with the rapid heating rate were used to study the reason that yields fast melting in each cycle of PCR [36], Results revealed that both the targets could be amplified and quantitated at the same time using an intercalating dye. Active cooling and heating is obtained by placing the sample chamber above the heat exchanger. During cooling, the hot fluid initially present is replaced by a valve of a refrigerant. Wheeler et al. used water as a fluid that passes from a porous matrix which works as a heat exchanger device [37]. A 5 micro liter sample could be cooled and heated at a rate of up to 45 ° C/s, giving reaction times of up to 45 ° C means less than 1 minutes per 10 cycles.

Another approach that uses a propylene glycol and water mixture which flows in a second chamber above the 25 micro liter sample chamber [38]. After the reinforcement, an analysis of the melting curve was carried out by creating a temperature difference to the cooling fluid in the tank. The capillary tubes were also used to perform PCR in the time domain. Sandburg et al. [40] nL placed PCR samples in fused silica capillary out of the eight tubes [39]. Active cooling is achieved with the help of the fan that can achieve the 50 ° C/s heating rate and 20 ° C/s cooling rate, It takes more than 12 min for a complete PCR, after that the flow can be processed further and samples can be extracted. Another approach has prepared a sample of 14 micro liter in the chamber having vent channel [40]. Chamber fills continuously as the resistance to flow is increased which also causes the sample to flows into the capillary bypass.

Heating and cooling has effectively done the utilization of two Peltier components on both sides of the sample chamber. The distinctive techniques of heating and cooling have diverse properties. While some offers rapid rates of cooling and heating, some have higher precision and can deal with bigger example volumes. The determination of the heating technique must compare to the applications and necessities.

2.3.2 Approaches to PCR

In different PCR approaches for time domain PCR, the sample solution remains stationary, and the motion of the preliminaries can by stopped by combining to a surface. This permits the combining of PCR with the Microarray technology [41]. The authors carried out the nested PCR settled in a microfluidic chamber. When the PCR was complete, a nested PCR was performed with a portion of the primers attached covalently to the surface of glass. The glass surface was washed after the complete reaction has taken place and then filled with an intercalating dye which is a form of aqueous solution. Avian flu RNA could be recognized using the pattern of fluorescence signs, optically encoded, hydrophilic porous polyethylene glycol micro particles were used by Jung et al. to make the forward primers stationary for different micro RNAs. The fluorescence signal was demultiplexed by separating the code on the molecule, which would prompt the parallel evaluation of a few microRNAs. Qin et al. has built up a NOA81 [42] microfluidic device. The gadget comprised of a microfluidic chamber which conquered a Peltier component for heating and cooling. Since NOA81 hinders the PCR response, the creators have secured the device using the bovine serum albumin to avoid assimilation of the DNA polymerase amid the response.

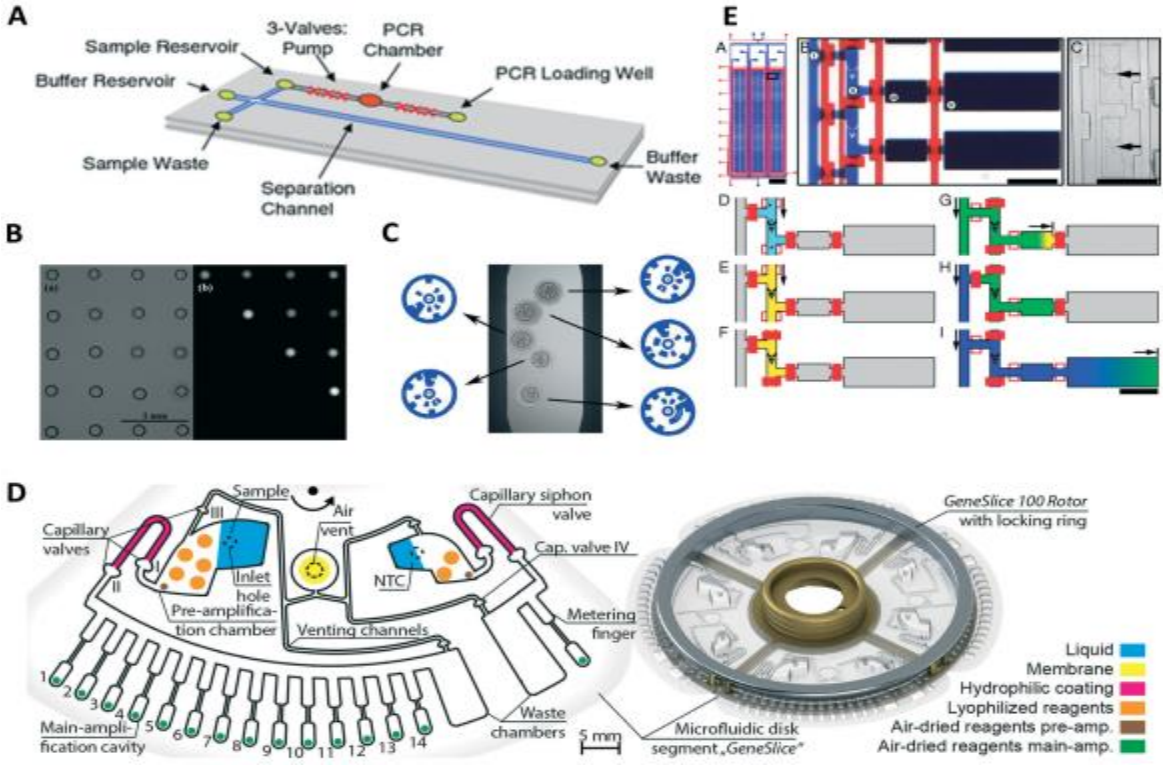

Figure 2.1: Various Time domain PCR devices.

(A) This device can perform PCR on blood samples taken from the whole body. Microfluidic valves are placed along with the PCR chamber for pumping action. After the samples have been amplified the targets are separated by the process of capillary electrophoresis performed on the same device.

(B) It shows a bright image of droplets on the left side and on the right side, it is an amplified representation of those droplets with the help of an infrared laser .This technique allows the application of unique temperature profiles to every individual droplet and also can reduce the testing to the selected droplets only.

(C) It shows a bright field image that includes the particles barcoded with the hydrogel, these particles are attached with the primers for various microRNAs which are bounded to them in microfluidic PCR device

(D) Various types of a centrifugal microfluidic device for nested PCR are shown on the left. The assembled centrifugal device for a commercial thermos cycler is illustrated on the right

(E) It shows the device used for the analysis of individual cells using reverse qrt PCR (a–c). Individual cells are confined in cell traps (e) prior to the washing and cell lysis step (d–f). Samples are made to flow into a reverse transcription chamber with the help of active valves (g and h). At last qtr. PCR is performed in a chamber (i)

2.3.3 Integrated devices

Some of the applications are focused on heating strategies or adjustments of the PCR procedure, several publications were focused on combining the, time domain PCR, preparation of the sample and post-PCR investigation. Ma et al. carried out a lysis venture in a chamber associated with two horizontal chambers [43]. When all the cells have been lysed the lysis buffer was replaced due to diffusion from the chamber walls using a PCR solution. Designers also took the advantage of difference in diffusivity between the PCR inhibitors and the long DNA strands of the solution in the same step. Thermolysis was performed in the chamber to separate DNA from Helicobacter pylori by combining them with magnetic particles. The magnetic particles stayed in the chamber for a few washes and consequent filling the chamber with the ace PCR blend [45]. After PCR, effective enhancement was affirmed by employing fluorescence measuring techniques

that utilizes the green interpolation color SYBR I. The DNA was separated with the help of magnetic beads prior to the discharging of into a microfluidic amplification chamber [46]. After enhancement, they were investigated. The objectives are utilized by capillary electrophoresis in a similar instrument. Membranes can likewise be utilized to separate DNA from a cell lysate. The human blood lysate was prepared utilizing a commercial item before the lysate was brought into a microfluidic device [47]. Silica gel was used to extricated DNA from the lysate .DNA is exchanged to another chamber for PCR. The continuous recognition empowered the extraction of amplification curves for evaluation, the analysis of the fusion curve was carried out. A coordinated layer was utilized at the passageway of the PCR assembly of a microfluidic device for extracting DNA [48].

Once the lysis is complete the DNA is held in the membrane where it is washed and dried prior to filling the chamber with master PCR blend discharging the held DNA. DNA was obtained from saliva using an aluminum oxide membrane samples in a microfluidic device. Samples are introduced in the device were they flow across the membrane, a short time later response blend was poured in to wells, where the PCR was performed. Di-electrophoresis was utilized to catch blood pathogens from slip chip having individual groves [50]. After separating the pathogens, a washing step was carried out using water to expel PCR inhibitors. In the feed channel slits were separated from the channel and heating was used to lyse the cells. The slide chip comprised of four parallel channels for sample preparation, taking into consideration the parallel discovery of four distinct pathogens.

Electrophoresis is the movement of charged particles with respect to a liquid brought about by an electric field. Velocities of the particles are dependent on net flux and size of the particles, which can also be used for the separation of particles. In this manner, electrophoresis is regularly utilized for post intensification investigation as plate gel electrophoresis. Scaling down of piece gel electrophoresis is frequently performed with the help of capillary electrophoresis (CE) which can accomplish higher detachment execution because of the higher surface area to volume ratio that neutralize the heating process of Joules. As capillary electrophoresis is an effective strategy for post intensification analysis, different coordinated time domain PCR devices are created. Le Rouxet al. utilized the heating from an infrared laser to perform PCR [51]. Samples that needed to be amplified were injected with microfluidic device, and the amplicons were segregated on the

basis of their length. Such combination strategy was utilized to evaluate short tandem repeats. Manage et al. utilized a capillary electrophoresis microfluidic device after intensification to isolate and distinguish amplicons [52]. As beginning PCR from entire blood for this situation, the CE detachment step is important to perform discovery of fluorescence after the enhancement response. This methodology has an advantage that intercalating dyes can be utilized and targets can be distinguished by length. Including the valve pump to the device eliminates the requirement for a pump from an external source, a variant, intersecting PCR was combined to a PCR chamber along with the set of CE channels [53]. After every cycle of PCR, a sample could be extracted from the chamber for further analysis using CE. This causes the real-time detection of PCR and also their numbering. Separation can be done in each detection step, and this device can monitor various amplification procedures in parallel along with the usage of a single intercalating dye.

2.3.4 Centrifugal microfluidic devices

In Centrifugal microfluidics, the centrifugal force and Coriolis Effect is used to spread the liquid in the radial directions. Because of their size, the design of the microfluidic devices is in the form of (CDs) Accessibility of a centrifugal microfluidic device based on CD, which can be a potential possibility for purpose of-care applications. A silicone/glass sandwich plate with 24 channels and 313 Micro Caminos with volumes of 1.5 nl were utilized to tally Salmonella enterica [54]. Solution composed of cells was placed in the input port and was dispersed using the radial force of micro cameras, which prompts a dispersion of Poisson microbes in the micro wells. PCR was started by thermal cycling through the disc. After the PCR, the amplified micro wells were counted to get the initial number of cells.

A device similar to this was utilized for reverse transcription of PCR [55]. The immediate reverse transcription of RNA was conceivable using a strong polymerase of DNA that is resistant to reticence. The placement of ice valves next with the PCR chamber allowed the other device materials to be used as well, for example, polycarbonate [56]. The liquid was solidified beside the chamber for PCR that forms a plug sealing causing the chamber to prevent evaporation of the sample. The "Lab Disk" format was developed at the Freiburg University located in Germany which offers various diverse capacities incorporated into a single disc, from test planning to examination after amplification

.The Lab disc comprises of four units, which demonstrates that allows the sample to be subdivided into eight halfway volumes (2D) [57, 58]. The dried reagents for the PCR response are discharged

from the samples in the chambers. The thermo cycling happens in a business thermos cycler. This was then changed to permit positive control without layout control or standards [59]. Changes have been made without trading off the capacity of the plate to fit in with a commercial thermos cycler, and without including the Pipetting steps. This technique was later used for the forensic identification of animal family [60]. It was also modified further to make the design compatible with the “Lab Disk Player”, a barrier was added to limit the vapor diffusion and pressure in the system that may rise due to the boiling of the PCR solution,

a vapor dissemination boundary was added to the framework to restrain the pressure in the framework, which can emerge due to the boiling of PCR solution [61].

The barrier was created for vapor diffusion by including a pressure chamber filled with air closer to the rotation center as compared to the PCR chamber. In the event of gas arrangement in the PCR chamber, the pressure is noted from the chamber, thus anticipating undesired pumping action of the solution. This "Lab Disk" was stretched out with DNA extraction capacities, permitting the necessary steps for the preparation to be carried out by the device. DNA extraction and washing, multiplexed PCR and discovery.it enables the process to be carried out with minimum handling costs. The advancement of the centrifugal devices is especially intriguing as they provide integrated devices with few handling steps.

2.3.5 Arrays

The samples are made stationary in space domain of the PCR device, the samples can be encoded at their respective spatial position within the arrays for various applications. Samples are imprinted in a water-oil emulsion in a Petri dish with test volumes in the scope of Nano liters [63]. The sample arrays was set up by contact printing method with the help of standard pipette tips. Infrared laser are used to heat the individual droplets, the cooling is achieved by the surrounding oil. In another method, a solution containing cells was circulated by a pipetting robot on a surface with hydrophilic spots [64]. The drops were immersed in mineral oil to prevent evaporation. The cells caught in droplets were lysed prior to adding of the reagents for reversed transaction of the pipetting robot. Xu et al conducted PCR in a device that was partitioned with the help of centrifugal device [65]. Targets are identified after the amplification process with the help of an array having probes of DNA printed for distinct targets on aldehyde-modified glass slides.

2.3.6 Single Cell devices

Several diseases are caused due to few abnormal cells. The microfluidics offers extraordinary potential outcomes to tackle this issue in light of the fact that the cells can be further divided into little volumes. The microfluidic devices combines the isolated cells with the PCR to examine the individual cells. The individual cells were printed in commercially available PCR tubes [66]. A Vacuum seal combined with the microfluidic inkjet technique was to ensure the distribution of cells containing droplets in the tubes. In another approach, the individual cells in a cell were detected through the cell trapping unit [67]. A chemical lysis step was performed and the RNA was captured by oligoIJd T) magnetic beads. After the beads were placed in a chamber for PCR, a transcription PCR was reversed. The effects of methyl methane sulfonate on a single human cancer cell could be tested. Lim et al. Cells encapsulated in individual droplets [68]. The droplets were gathered in a vial and PCR was performed in a benchtop PCR using Taq Man tests. The droplets were introduced into a droplet classifier where the drops showing the positive amplification were separated for the recovery of complete genome of the cells .The cells can also be isolated by pneumatic valves in microfluidic devices. The cells can likewise be detached by pneumatic valves in microfluidic frameworks. The framework takes into account the simultaneous capture and transcription by PCR in a 96x96 [69, 70] system. Another valve-based structure had 300 cell traps in chambers isolated by valves81. The reverse transcription chamber can be employed for chemical lysis of cells when a “one pot” reverse transcription PCR was carried out in the PCR chamber.

2.4. Problem Statement

After studying the number of research articles about space domain microfluidic devices and time domain PCR devices, the most research article deal very small amount of fluid sample up to 20 microliter. The main focus of this thesis to design a sample block for 50 microliter fluid sample, and the other main concern of this research to design sample bock with lowest possible mass therefore it give quick response of temperature.

The focus of this thesis to make a design of sample block for 50 µl and then investigate the thermal response of sample block. During analysis they also investigated the effect of mass on temperature response and energy consumption.

The specific objectives of this thesis are outlined as follow:

i. To determine the effect of Sample Block mass on supplied energy.
ii. To investigate the effect of mass on temperature response of device.
iii. To determine whether 50 µl Sample Block device will be able to resolve the longstanding problem of thermal cross-talk.
iv. To investigate the species transport in Peltier heating PCR device for a better understanding of kinetic mechanisms.

2.4.1. Advantages of Static Chamber Microfluidic Device over other technologies

The advantages of employing miniaturize static chamber PCR are as follow:

i. Low wear and tear because no moving component in this proposed device.
ii. Very high heating and cooling rate by using Peltier heating & cooling element.
iii. Less bulky device.
iv. Quick response and energy efficient design by mass optimization
v. Device portability and accessibility.
vi. Simplify overall reaction
vii. Cost effective mass production of miniaturize PCR.
viii. Easy manufacturing of Sample Block with just CNC and EDM wire cut.
ix. Work for large sample size as compare to available in research

CHAPTER 3

DESIGN OF POC (POINT OF CARE) DEVICE

3.1. Design of Sample Block

The different style of PCR devices are available in market. SC-PCR device presented in this study have number of parts, such as (a) Aluminum Sample block (b) Polyethylene tube (c) Peltier heating/ cooling device (d) Heat sink.

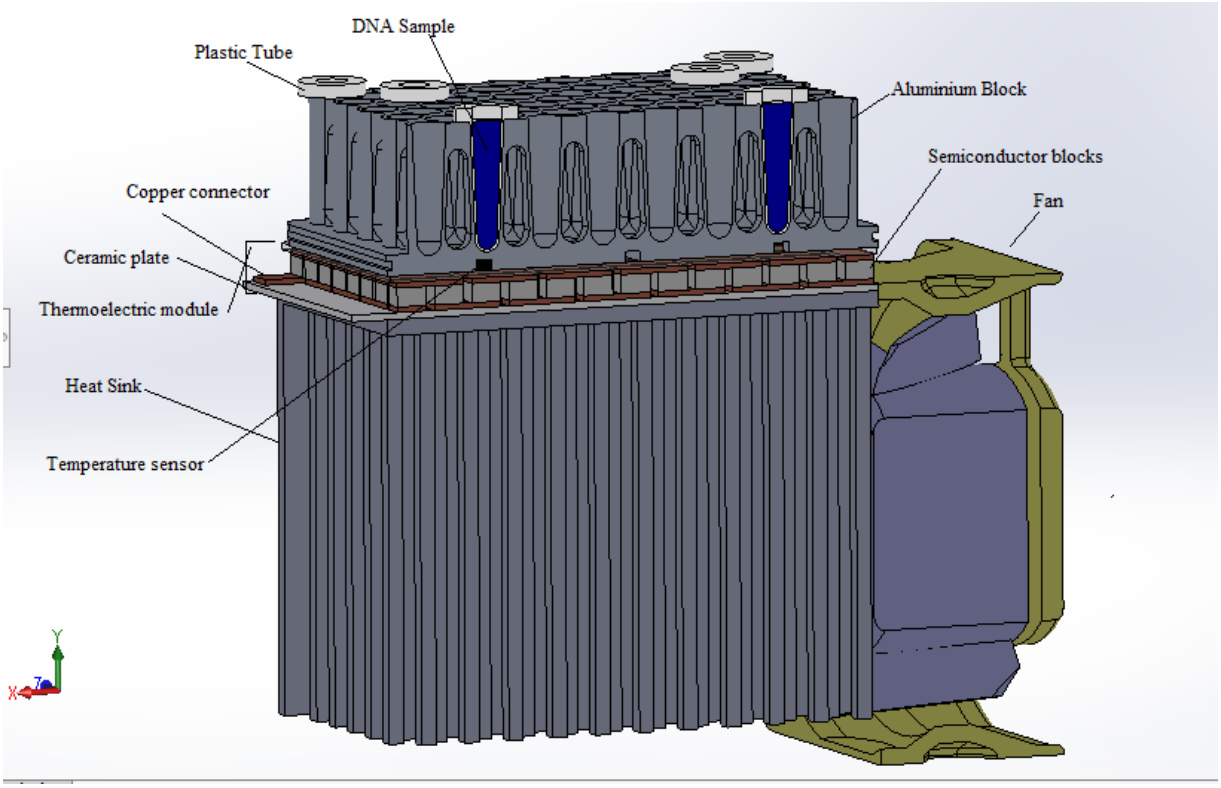

Figure 9.1: PCR Device

Here main purpose of design is to minimize the mass of device therefore its required

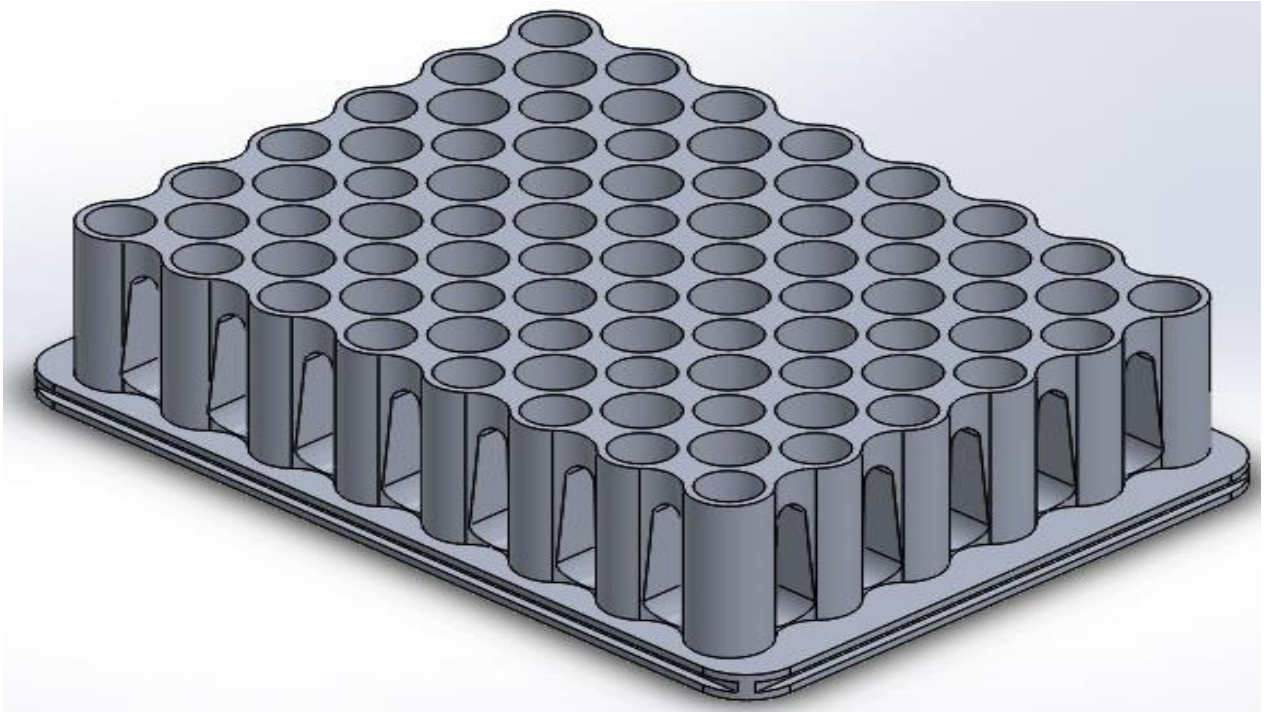

Figure 3.2: Aluminum well type Sample Block

minimum energy to get required temperature. The current device is feasible for 50+ microliter sample as shown in below.

The present design of sample block is suitably rigid in construction to provide flat solid base for secure contact with thermoelectric modules and effective heat transfer. The heat conducting sample block with high thermal conductivity, low heat capacity and good mechanical strength. As the mass of blocked is reduced the speed of heating and cooling of block is maximized. Its 48 well sample block and polyethylene tubes are used for DNA sample which fit inside the wells of block. The number of blind holes done from top surface of block and taper slots on side of block to achieve minimum mass. The elliptical slots are made parallel to top and bottom surface of sample block. The sample block provide the maximum contact surface area to the sample plate (disposal plate in some time), as the contact surface area increase the heat transfer increase and reduce the time of test. The center to center distance of sample tube holes is 6 mm. the current design of sample block have 48 (6×8) well and each well have capacity 50 microliter. The height of sample block is 14 mm.

The sample block good to make in one piece construction, its mean the block is manufacture by molding or machining in single piece rather than by joining the sheets. The sample block is rigid and prefer to make by material which have high thermal conductivity and stiffness properties. The suited material for the sample block is copper, silver, iron, magnesium and aluminum and other alloy, but in this study for thermal analysis of sample block aluminum material is used. The sample block have rectangular array of wells, the wells evenly spaced.

3.2. Design of Polyethylene Tubes

The tubes are designed for 1 to 50 microliter liquid DNA solution in volume. Here it is desirable to minimize the temperature differential with the volume of an individual sample during thermal cycling process. The temperature uniformity effected as the liquid sample increase, and required more time to attain the required temperature. The tube generally thin section which have thickness 0.5 to 0.75 mm, because it's plastic material which have very low thermal conductivity. The tubes are made in taper therefore make good contact with aluminum block wall by applying force on top and transfer maximum heat. The tubes are arranged in 6 by 8 matrix as well block. Here can be use single tube.

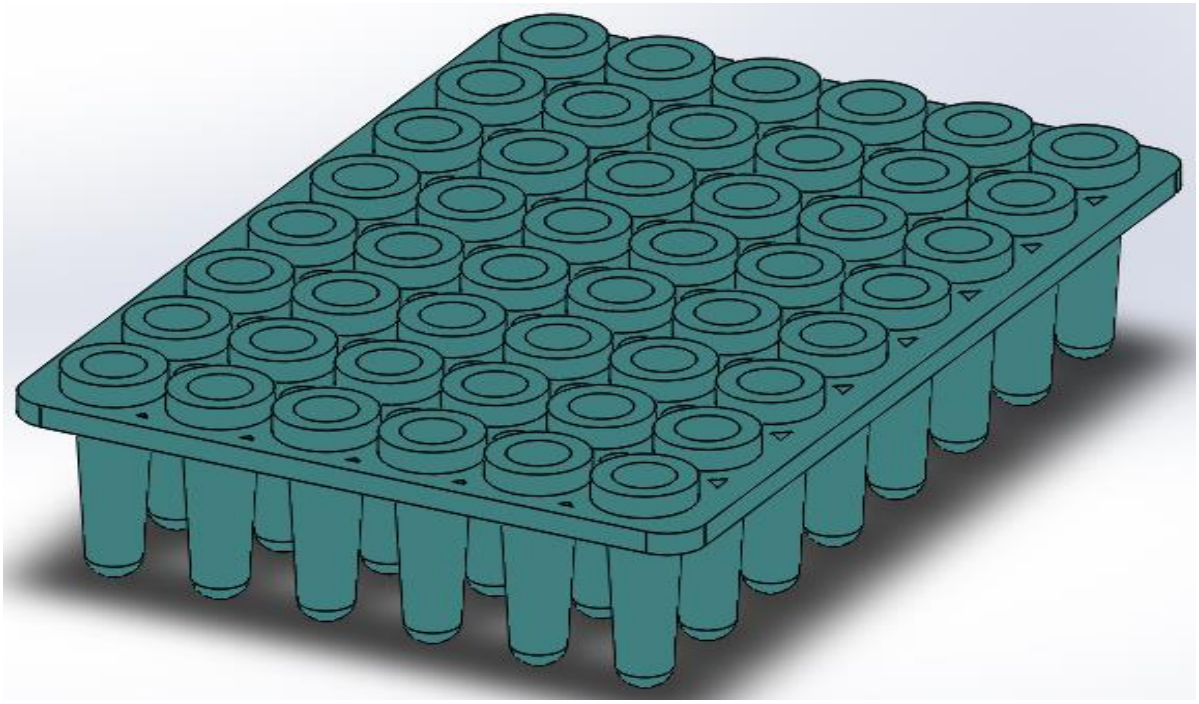

Figure 3.3: Tubes

3.3. Design of Thermal Electric Module (Peltier)

There are different way to get required temperature of block, but for DNA amplification required cyclic temperature in which need to increase and decrease temperature so here need such device which can produce both effect to reduce the cycle time. For this purpose the thermoelectric (TE) device used in this model. The n-type semiconductor and p-type semiconductor are heavily doped with electrical carriers which used in thermoelectric module. The elements are arranged in such way these are connected series electrically but thermally in parallel pattern as shown in figure.

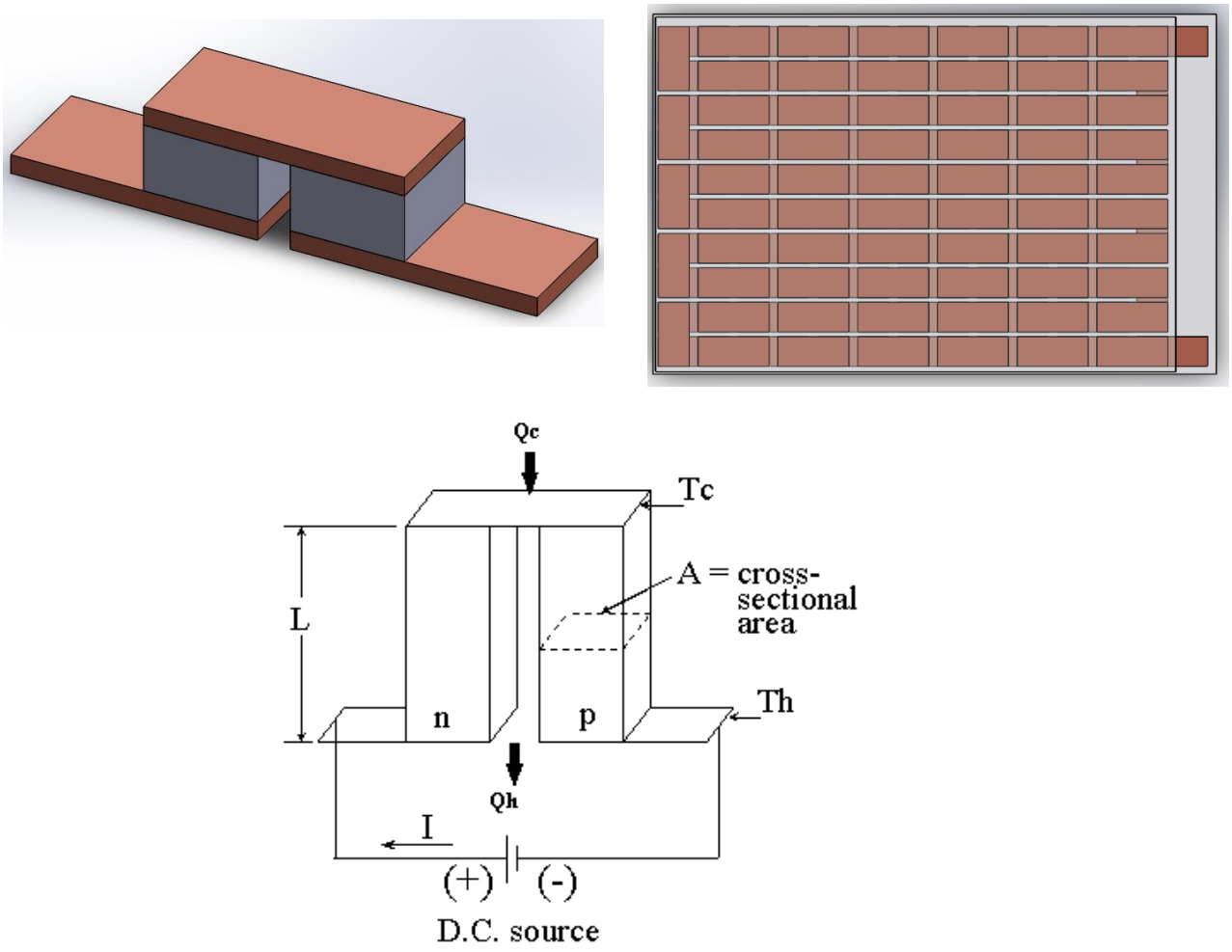

Figure 3.4: Solidwork Thermo Electric Module model and its features

The thermoelectric module is solid state heat pump that on that work Peltier effect (cooling effect is generated as the electric current pass through junction of two dissimilar material, and when

changing the direction of current it's generate the heating effect). The Peltier is consist of couples of these type of junctions. The TE element which used in this research have 70 couples. The specification of cyclic thermoelectric module get from Marlow product specification data catalogue.

There are some advantage to select the Thermo Electric Module (Peltier) for heating and cooling purpose in following study.

No Moving Parts: A thermoelectric module works without making use of any moving parts. It works electrically. This is why they do not require any maintenance.

Small Size and Weight: As compared to mechanical system, the thermoelectric cooling system is far more efficient, small and light in weight. It is also very compatible and has a lot of variety. It comes in a lot of sizes and configurations. So, there are almost zero non-compliance issues to meet application requirements

Ability to Cool below Ambient: When a TE cooler is attached with a heat sink, it works wonders. It has remarkable capacity to reduce temperature quite effectively. Whereas, a conventional heat sink alone takes a lot of time to cool down.

Ability to Heat and Cool with the same module: The cooling or heating effect of a thermoelectric depends on polarity of applied DC source. This enables us to eliminate extra heating and cooling units.

Precise Temperature Control: In a temperature controlled closed-loop circuit, TEs are best. TE coolers can control temperatures upto +/- 0.1°C

High Reliability: Thermoelectric modules are very reliable. Their reliability is mainly because of solid state build quality. Reliability is a subjective topic and it is also application dependent on application but typical life of TE cooler is more than 200000 hours.

Electrically "Quiet" Operation: TE modules are very much noise proof. They create almost no electrical noise and can be used in combination with sensitive sensors. This is quite the opposite for mechanical refrigeration systems.

Operation in any Orientation: TEs are very popular in many aerospace environments because they can be used in any orientation. They can also be used in zero gravity environments.

Convenient Power Supply: TE modules can be used directly from a DC power supply. Variety of modules with varying ranges of voltages and currents are available. Pulse width modulation (PWM) may be used in many applications.

Spot Cooling: TE cooler allows us to cool down a specific area or component. This way excessive loss of usage is avoided to cool down an entire package or enclosure.

CHAPTER 4

SIMULATION SETUP AND NUMERICAL METHODOLOGY

The first step of designing a TE heating and cooling system incorporates in depth study of thermal parameters of a system. To ensure an efficient and effective design, this in depth analysis must never be avoided no matter how simple or complex this is for some applications. The mathematical models of heat transfer, thermoelectric module and PCR amplification are also discussed below:

4.1. Heat Transfer model

Let here consider material is isotropic with temperature dependent heat transfer

The general heat equation is

$$\left(\frac{\partial q_x}{\partial x}+\frac{\partial q_y}{\partial y}+\frac{\partial q_z}{\partial z}\right)+Q=\rho c\frac{\partial T}{\partial t} \tag{1}$$

Here q_x, q_y, q_z is heat flow through the unit area

$Q=Q(x,y,z,t)$ Heat generation rate per unit volume

$\rho=$ Material density

$c=$ Heat capacity

$T=$ Temperature

The heat flux from Fourier law of heat transfer

$$q_x=-\frac{\partial T}{\partial x} \qquad q_y=-\frac{\partial T}{\partial y} \qquad q_z=-\frac{\partial T}{\partial z} \tag{2}$$

So general heat equation become as

$$\left(\frac{\partial}{\partial x}\left(\frac{\partial T}{\partial x}\right)+\frac{\partial}{\partial y}\left(\frac{\partial T}{\partial y}\right)+\frac{\partial}{\partial z}\left(\frac{\partial T}{\partial z}\right)\right)+Q=\rho c\frac{\partial T}{\partial t} \tag{3}$$

Following type of boundary conditions are applied in this research

i. Specified temperature

$$T_s = T(x, y, z, t) \quad (4)$$

ii. Heat flux boundary conditions

$$q_x n_x + q_y n_y + q_z n_z = -q_s \quad (5)$$

iii. Convection boundary condition

$$q_x n_x + q_y n_y + q_z n_z = h(T_s - T_e) \quad (6)$$

Here the convection coefficient is calculated as

ΔT =Difference between PCR and atmospheric temperature

β = Coefficient of Thermal Expansion

v = Kinematics viscosity

$T_{\max} = 95 + 273.1 = 368K$

$T_{\min} = 55 + 273.1 = 328.1K$

$T_{avg} = \frac{328 + 368}{2} = 348K$ $\qquad T_{amb} = 25C^0 = 25 + 273.1 = 398.1K$

$T_{film} = \frac{T_{avg} + T_\infty}{2} = \frac{75+25}{2} C^0 = 50C^0 = 50 + 273.1 = 323.1k$

$$\beta = \frac{1}{T_{film}} = \frac{1}{323.1} = 0.003095$$

$v = 1.91 \times 10^{-5} m/s^2$ At average temperature

$L = 0.013m$

Grashoff Number (Gr)

$$Gr = \frac{g\beta(T_s - T_\infty)L^3}{v^2} \quad \textbf{(7)}$$

$$Gr = \frac{g \cdot \beta \cdot \Delta T L^3}{v^2} = \frac{9.81 \times 0.003095 \times 50 \times 0.013^3}{(1.91 \times 10^{-5})^2} = 9142.40$$

After substituting values in above equation we get

= 9142.4

Prandtl Number (Pr)

Air properties at atmospheric temperature and pressure given below

$\rho = 1.1644 kg/m^3$

$\mu = 1.865 \times 10^{-5} kg/m-s$

$k = 2.638 \times 10^{-2} W/m-{}^oC$

$c_p = 1.00064 kJ/kg-{}^oC$

$$\Pr = \frac{\mu c_p}{k} = \frac{1.8651 \times 10^{-5} \bullet 1.00064 \times 10^{-3}}{2.638 \times 10^{-2}} = 0.701 \quad (8)$$

Rayleigh Number (Ra)

$$Ra = Gr \times \Pr \quad (9)$$

The values of Rayleigh number by putting the Grashoff number and Prandtl number in above equation

= 6408.86

Nusselt Number (Nu)

For vertical plate a correlation that may be applied over the entire range of Ra has been recommended by Churchill and Chu and is of the form

$$Nu = \left\{ 0.825 + \frac{0.387 \bullet Ra^{1/6}}{\left[1 + \left(0.492 / \Pr \right)^{9/16} \right]^{8/27}} \right\}^2 \quad (10)$$

Substituting the value of Ra in the above formula

We get,

$$Nu = \left\{ 0.825 + \frac{0.387 \cdot (6408.86)^{1/6}}{\left[1 + \left(0.492/0.7\right)^{9/16}\right]^{8/27}} \right\}^2 = \left\{0.825 + \frac{1.629}{1.19409}\right\}^2 = 4.793$$

$$L_c = \frac{4wL}{2(w+L)} = \frac{0.015}{0.25} = 0.06$$

Convective heat transfer coefficient (h)

$$Nu = \frac{hLc}{K}$$

$$h = \frac{4.793 \times (0.0273)}{0.06} = 2.18 \frac{W}{m^2 k} \quad (11)$$

Coefficient of heat transfer of convection from sides and top is $2.18 W/m^2.\mathrm{k}$ and we considered the value of coefficient of heat transfer in this thesis 3. The radiation effect is neglected here.

4.2. Thermoelectric Module Numerical modeling

The mathematical model of thermoelectric module described here. The semiconductor material have many temperature dependent properties. Here algebraic expression are given to simulate the performance thermoelectric component.

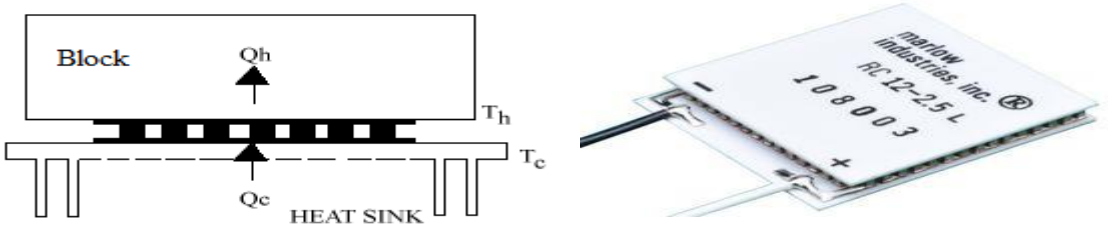

Figure 4.1: Peltier

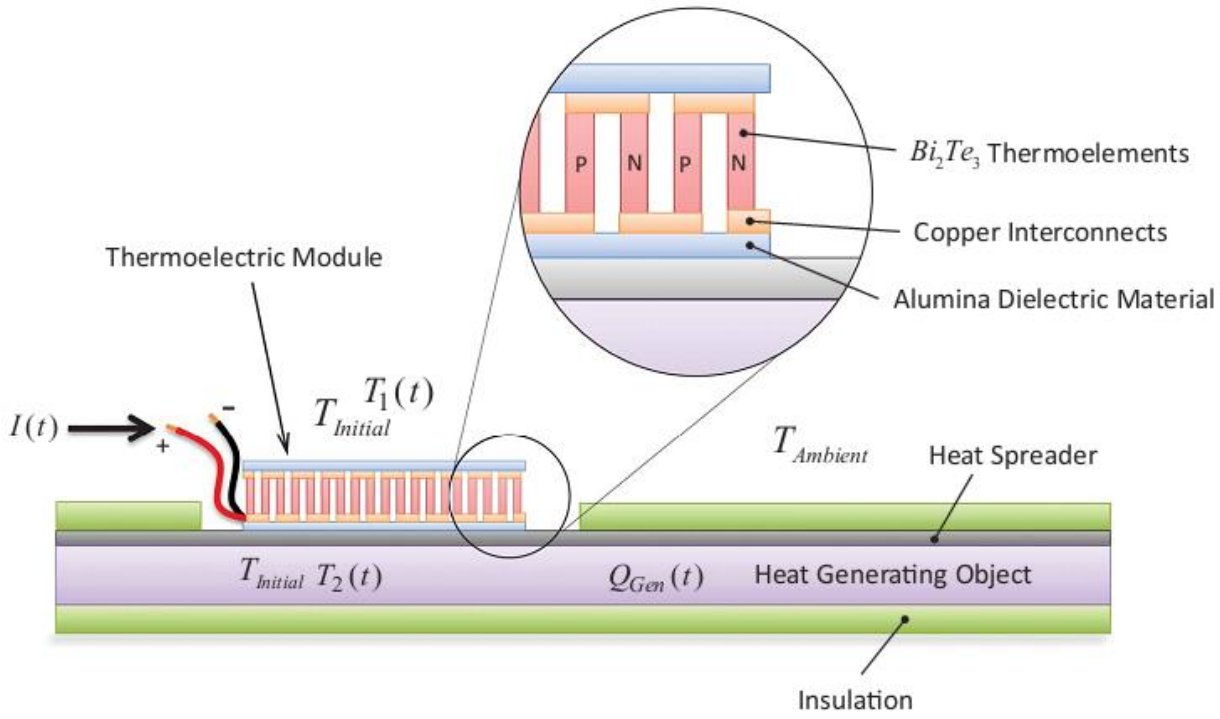

Figure 4.2: Peltier Working and parts

The governing equation of one dimensional transient heat transfer by applying an energy balance analysis for the P-type element. [12]

$$\frac{\partial^2 T}{\partial x^2} - \frac{I\tau}{AK_M}\frac{\partial T}{\partial x} + \frac{I^2 R_M}{A^2 K} = \frac{\rho C_p}{K_M}\frac{\partial T}{\partial t} \tag{12}$$

The boundary condition for transient P type element as follow

$$K_M \left.\frac{\partial T}{\partial x}\right|_{x=0} = \frac{Q_c}{A} = q_c$$
$$K_M \left.\frac{\partial T}{\partial x}\right|_{x=L} = T_h \tag{13}$$

And the steady state equation for the thermoelectric element as given below

$$\dot{Q}_h = n\left[(S_m \times T_h \times I) + (0.5 \times I^2 \times R_m) - (K_M \times (T_h - T_c)\right] \quad (14)$$

$$\dot{Q}_c = \left[(S_M \times T_c \times I) - (0.5 \times I^2 \times R_M) - (K_M \times DT)\right] \quad (15)$$

The rate of work done by thermoelectric module is calculated by an Energy balance equation around the boundary

$$\dot{W}_n = \dot{Q}_h - \dot{Q}_c \quad (16)$$

By substituting above equations work done of thermoelectric module can be get as

$$\dot{W}_n = \left[S_M I \times DT\right] + I^2 R_M \quad (17)$$

Required input voltages are

$$V_{in} = \left(S_M \times DT\right) + \left(I \times R_M\right) \quad (18)$$

The maximum and operation value of Current is as

$$I_{\max} = \frac{S_M}{R_M}\left[\left(T_h + \frac{1}{Z}\right) - T_h^2\right]^{0.5} - \frac{1}{Z}$$
$$I_{opera} = \frac{S_M T_h}{R_M} \quad (19)$$

Here DT is temperature difference between hot and cold side

$$DT = T_h - T_c \quad (20)$$

4.3. PCR kinematics

The polymerized chain reaction (PCR) DNA amplification is very complex process with handful of details are available for chemical reactions that are involved in three steps of PCR. The PCR kinetic model adopted in this study to formulate and estimate kinetic parameters is proposed by

Hunicke-Smith [129]. The chemistry model consists of five major chemical species which control the reactions in denaturation, annealing and extension zones. There are not many detail available of chemical reactions of 3 process of PCR DNA amplification

Denaturation $$S_1S_2 \xleftrightarrow[K_D^-]{K_D^+} S_1 + S_2 \quad (21)$$

Annealing $$S_1 + P_2 \xleftrightarrow[K_A^-]{K_A^+} S_1P_2$$
$$S_2 + P_1 \xleftrightarrow[K_A^-]{K_A^+} S_2P_1 \quad (22)$$

Extension $$S_1P_2 \rightarrow K_E S_1S_2$$
$$S_2P_1 \rightarrow K_E S_1S_2 \quad (23)$$

The chemical reaction presented in equation (19) show the splitting of double strand DNA (dsDNA) S_1S_2 into single-stranded DNA (ssDNA) S_1 and S_2. In the annealing process the forward and reverse primers P_1 and P_2 bind on single stranded DNA to generate complexes of both in form of S1P2, P_1S_2. The fourth and fifth chemical reaction presented in extension presented to make new amplified DNA. These reaction show the amplification of DNA in form 2^n.

The concentration of these five chemical species change with time so the concentration rate equations given as

$$\frac{d(S_1)}{dt} = K_D^+[S_1S_2] + K_A^-[S_1P_2] - K_D^-[S_1][S_2] - K_A^+[S_1] \quad (24)$$

$$\frac{d(S_2)}{dt} = K_D^+[S_1S_2] + K_A^-[S_2P_1] - K_D^-[S_1][S_2] - K_A^+[S_2] \quad (25)$$

$$\frac{d(S_1P_2)}{dt} = K_D^+[S_1] - K_A^-[S_1P_2] - K_E[S_1P_2] \quad (26)$$

$$\frac{d(S_2P_2)}{dt} = K_D^+[S_2] - K_A^-[S_2P_1] - K_E[S_2P_1] \quad (27)$$

$$\frac{d(S_2S_2)}{dt} = K_E[S_1P_2] + K_E[S_2P_1] - K_D^+[S_1S_2] - K_D^-[S_2P_1] \quad (28)$$

The backward and forward reaction rate constant are temperature dependent. Theses reaction rate constants equation proposed by Hunicke-Smith [129] is as follow.

$$K_D^+(T) = \frac{K_o^+\left(1+\tanh\left[\frac{T-361}{5}\right]\right)}{2} \tag{29}$$

$$K_D^-(T) = \frac{K_o^-\left(1+\tanh\left[\frac{-(T-348)}{5}\right]\right)}{2} \tag{30}$$

$$K_A^+(T) = \frac{K_1^+\left(1+\tanh\left[\frac{-(T-335.5)}{5}\right]\right)}{2} \tag{31}$$

$$K_A^-(T) = \frac{K_1^-\left(1+\tanh\left[\frac{T-339}{5}\right]\right)}{2} \tag{32}$$

$$K_E(T) = K_2 \times \exp\left(-\left[\frac{T-345}{5}\right]^2\right) \tag{33}$$

Table: 4.1 Operational parameters of the species

Species	Initial concentration (mole/m^3)	Diffusion coefficient (m^2/s)
S_1S_2	5.71E-12	1.0E-10
S_1P_2 and S_2P_1	0	1.0E-10
S_1 and S_2	0	1.0E-10
P_2 and P_1	3.0E-7	1.0E-9

Here K_1^+, K_1^-, K_o^+, K_o^- and K_2 in that order equal to $5\times10^9 M^{-1}s^{-1}, 10^{-4}s^{-1}, 12.5s^{-1}, 10^9 M^{-1}s^{-1}$ and $0.32s^{-1}$, and the T is fluid sample temperature in C^o. The constant parameters of reaction rate

are basically depend upon temperature as shown in figure 4.3. The initial concentration, operation parameters and diffusion coefficient are given in table below. [130]

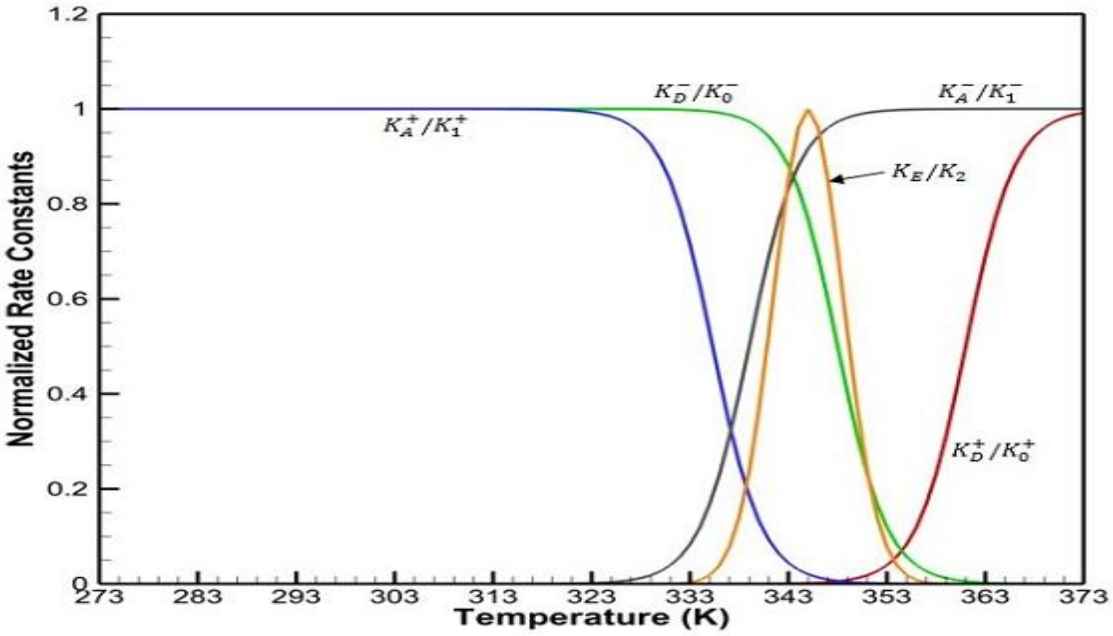

Figure 10.3: Effect of temperature variation on normalized reaction rate constants.

4.4. Simulation setup

Firstly the geometries of device are modeled in Solidwork 2018 and then the thermal analysis is done by using ANSYS transient thermal and steady state module. For analysis purpose firstly defined the materials and their properties as mentioned in above table. The temperature transient boundary condition is applied at base of device as it will work in real practice. As discussed in first chapter, there are three different temperature ranges (Denaturation 92-98 ^{o}C, Annealing 50-60 ^{o}C, Extension 68-72 ^{o}C) are required for specific time interval for PCR process. For the convection boundary condition, heat transfer convective coefficient is calculated and applied at the side walls and all other surfaces which are exposed to air. The heat transfer by radiation at all external surfaces are neglected. The study domain consist at the alumimum Sample block, plastic tubes to carry the sample , fluid sample (water properties) and glass cap, it's very large domain for calculation purpose. The density and dynamics viscosity of DNA sample is consider equal to water, and the density and dynamics viscosity is function of temperature from ANSYS fluid properties data Base. To reduce the computational cost the axis symmetric boundary is applied and get the one fourth domain.

CHAPTER 5

MODEL VALIDATION AND VERIFICATION

5.1. Mesh Sensitivity Analysis

Mesh sensitivity analysis is important while performing FEA transient thermal simulations. It tells about the authenticity and convergence of solution. Convergence of solutions depends upon the many factors i.e. correct boundary conditions and mesh independence. Correct number of elements and mesh type e.g. quadratic or hexagonal is also an important factor while performing the Ansys simulations. Mesh of one fourth part of Static chamber PCR device is shown in below figure. Total elements taken for the mesh are 90862. These are the acceptable number of elements for the current calculations. To reduce the computational cost the axis symmetry in applied and got one forth part of device. All calculations are done on this one fourth part of device.

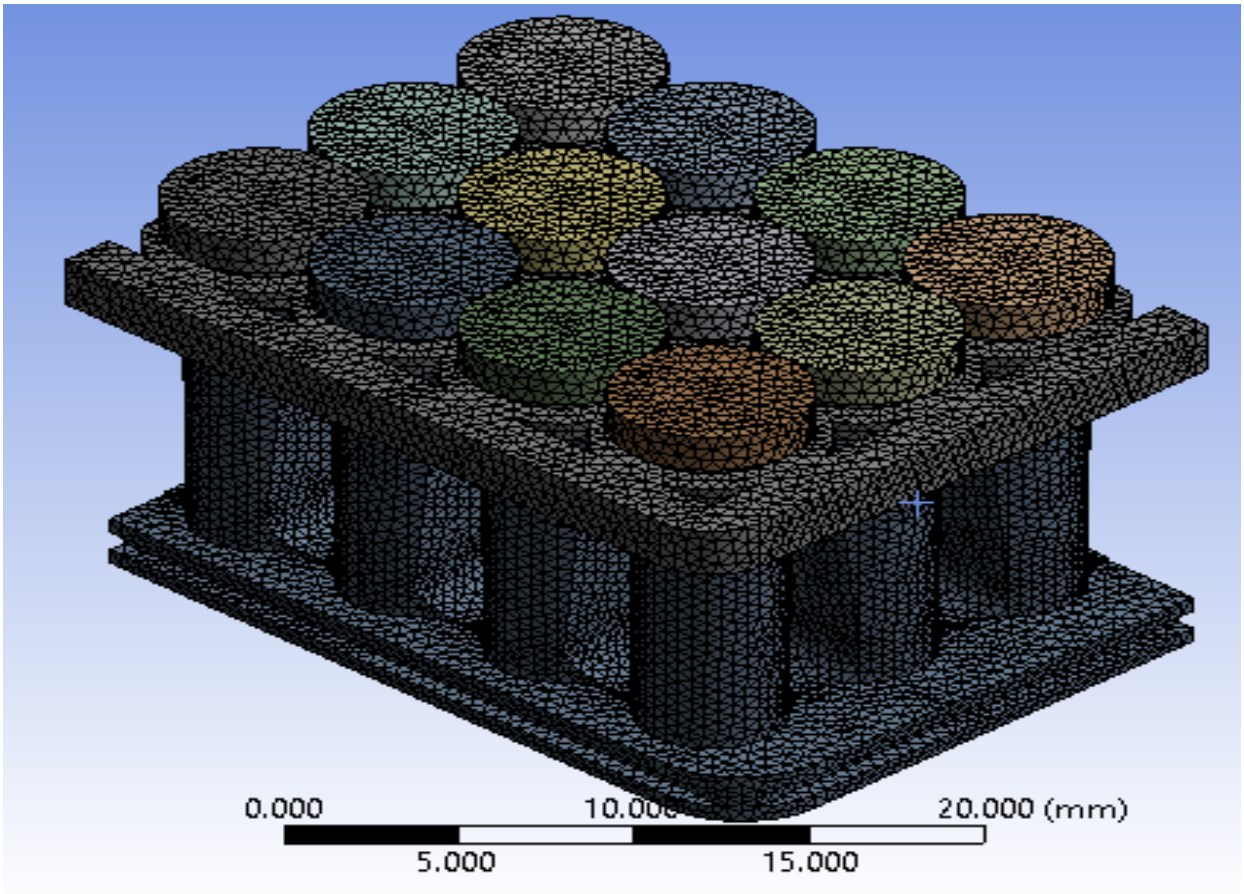

Figure 5.1: Quadratic Element meshing for FEA analysis

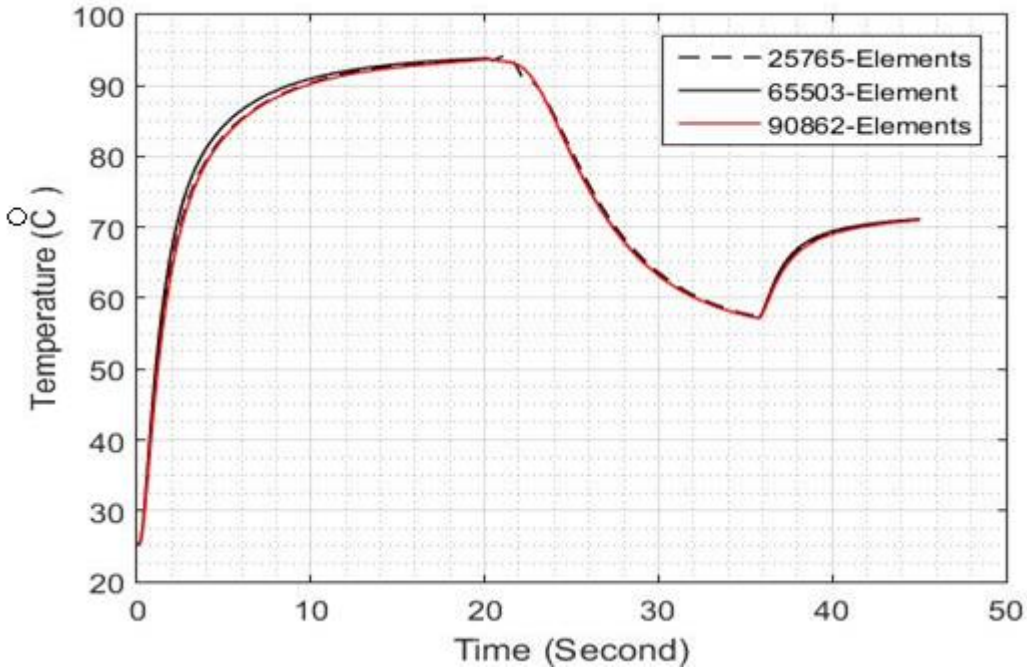

Figure 5.2: Temperature response at probe 1 at different number of elements

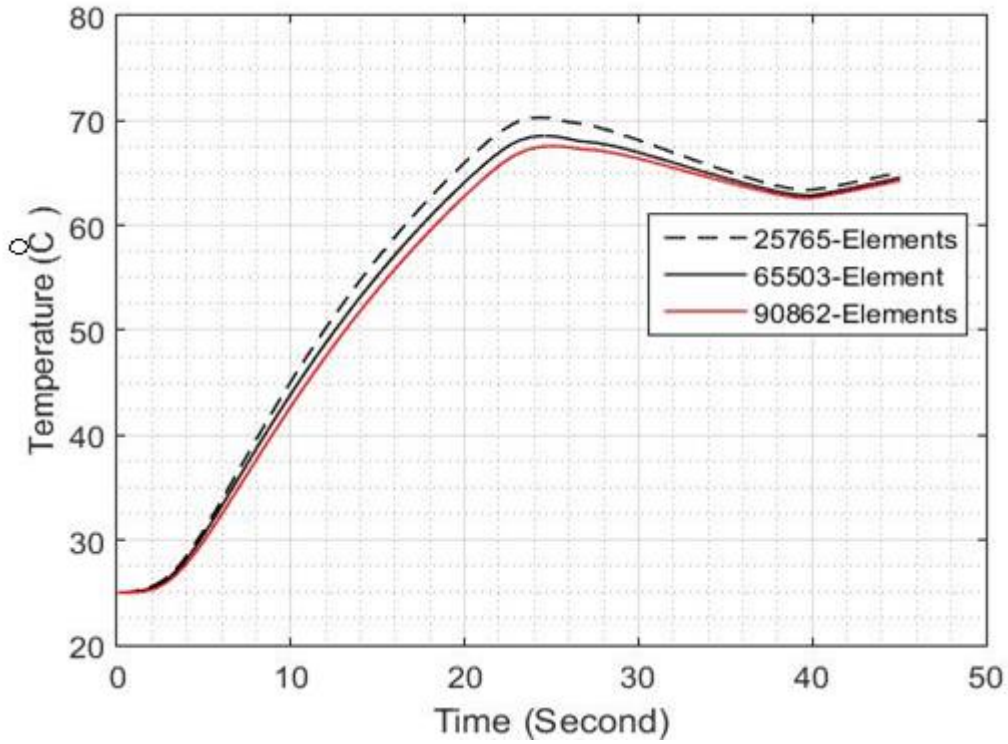

Figure 5.3: Temperature response at probe 2 with different number of elements

For the current simulations we took three different mesh sizes and performed simulations. Size of elements are shown in the figure 5.3. We choose mesh of 90862 elements because further refinement in this mesh have no effect on the desired output and results.

In the second step, mesh refinement of one-cycle computational model is performed to have good grid density quality. In one-cycle computational model, there are four domains: (i) aluminum Sample Block, (ii) polypropylenes tubes (iii) fluid domain and (iv) glass cap. By default meshes are generated with decreasing the mesh size and quadratic element order are used in this study. The one cycle is consisted at 45 second. The temperature boundary conditions are applied at the base of Sample Block. At the mesh size of 90862 elements error in the temperature profile is has become negligible and this temperature profile of this mesh size is suitable for our current calculations. Neumann boundary condition is applied at base of the sample block and the temperature response at two different point of domain is observed. The prob-1 at fluid domain and prob-2 at the glass cab of device. The temperature at prob-2 is low as compare to prob-1 because it's at outside of device where convection boundary conditions is applied.

5.2. Model Validation

The simulation setup is validated with the one dimensional analytical calculations, which show the same numerical results. The Temperature boundary conditions applied at base of Sample Block and noted how the temperature change. The below figure show the boundary condition of simulation and analytical calculation. Here was three layers of material, first one is aluminum block, Polypropylene tube and water.

For 1-D heat transfer analysis following equations are used for analytical solution. Differential equation for 1-D case is simply reduced to $K\frac{d^2T}{dx^2}+Q=0$

and the possible boundary conditions are $T=T_\infty$ $K\frac{dT}{dx}Ix+h(T-T_\infty)=0$

on the free surface. And 1-D stiffness matrix is calculated through the following equation.

$$k^{(n)}=\left(\frac{KA}{L}\begin{bmatrix}1 & -1\\ -1 & 1\end{bmatrix}+\frac{hPL}{6}\begin{bmatrix}2 & 1\\ 1 & 2\end{bmatrix}+hA\begin{bmatrix}0 & 0\\ 0 & 1\end{bmatrix}\right)$$

$$F^{(n)}=\left(\frac{hPLT_\infty}{2}\begin{Bmatrix}1\\ 1\end{Bmatrix}+hAT_\infty\begin{Bmatrix}0\\ 1\end{Bmatrix}-\frac{qPL}{2}\begin{Bmatrix}1\\ 1\end{Bmatrix}-qA\begin{Bmatrix}0\\ 1\end{Bmatrix}+\frac{QAL}{2}\begin{Bmatrix}1\\ 1\end{Bmatrix}\right)$$

In figure 5.4 a short part of PCR device is shown and following boundary conditions are applied. At the base a temperature of 95 degrees is applied and on periphery and top surface a convective boundary condition is applied with a convective heat transfer coeffiectint of value 5 w/m^2-k. While keeping ambient temperature 25 degrees. All these mentioned boundary conditions are applied to the original design for simulation purpose. Then we performed simulations using Ansys and compared the results with the analytical solution governed by the above given equations. A comparison of analytical and numerical values is shown below in the graph. Temperature profiles are almost same but with a small fluctuation at the end. This small fluctuation is caused may be due to the numerical schemes used in the Ansys to achieve convergence.

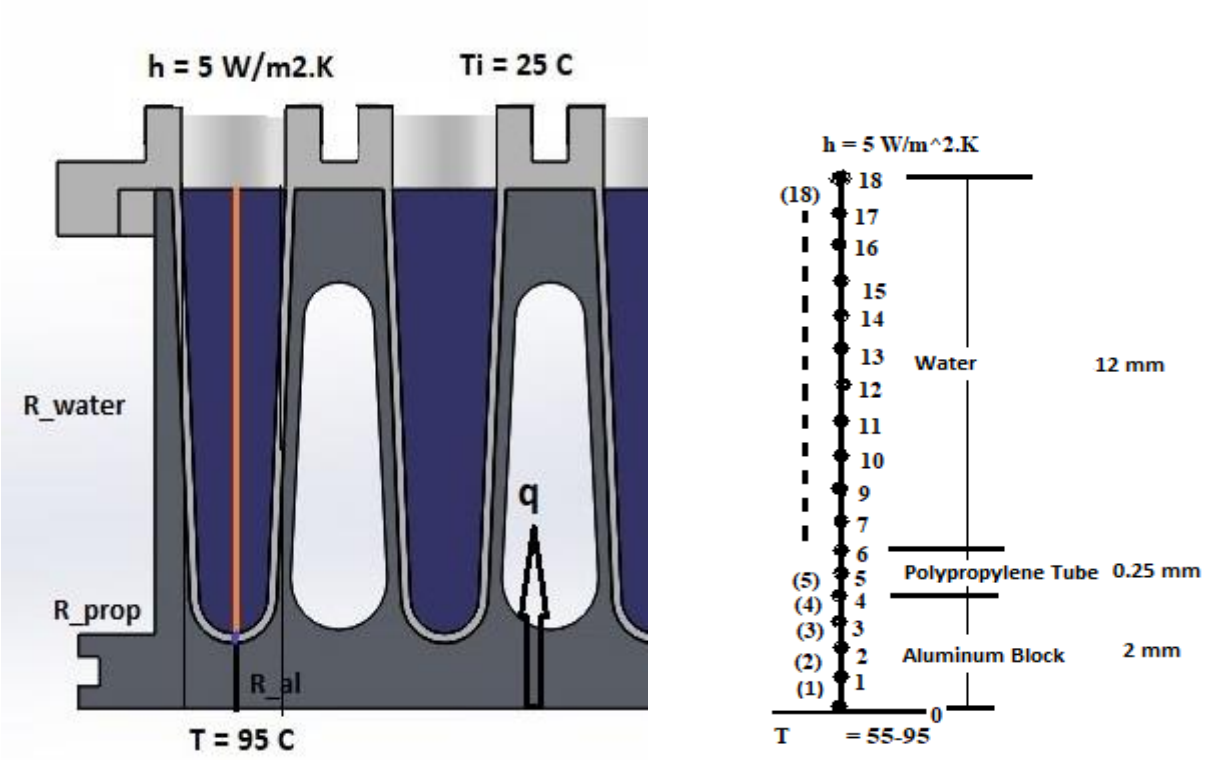

Figure 5.4: The boundary condition for validation of simulation setup

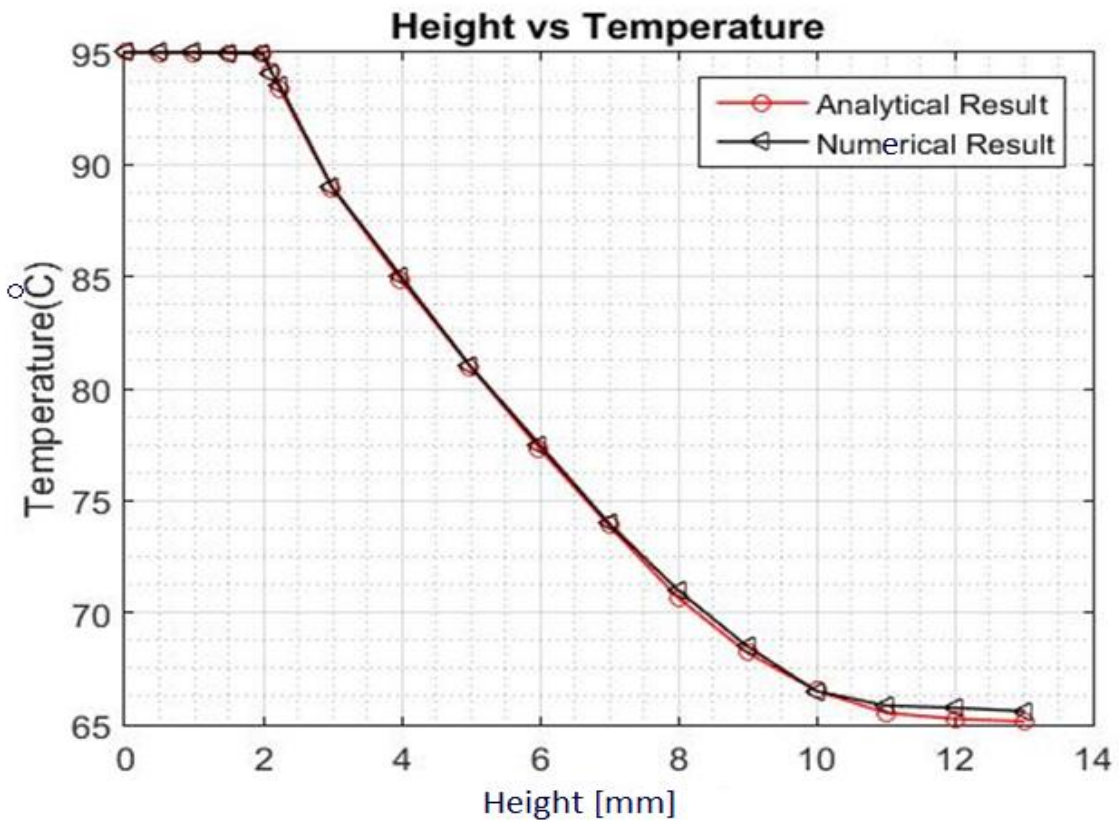

Figure 5.5: Results comparison of analytical and numerical study

5.3. Boundary Conditions

Following boundary conditions are applied to the design model.

1) Temperature BC
2) Convective BC
3) Adiabatic BC
4) Symmetric BC

All these Boundary conditions are shown in the figure below.

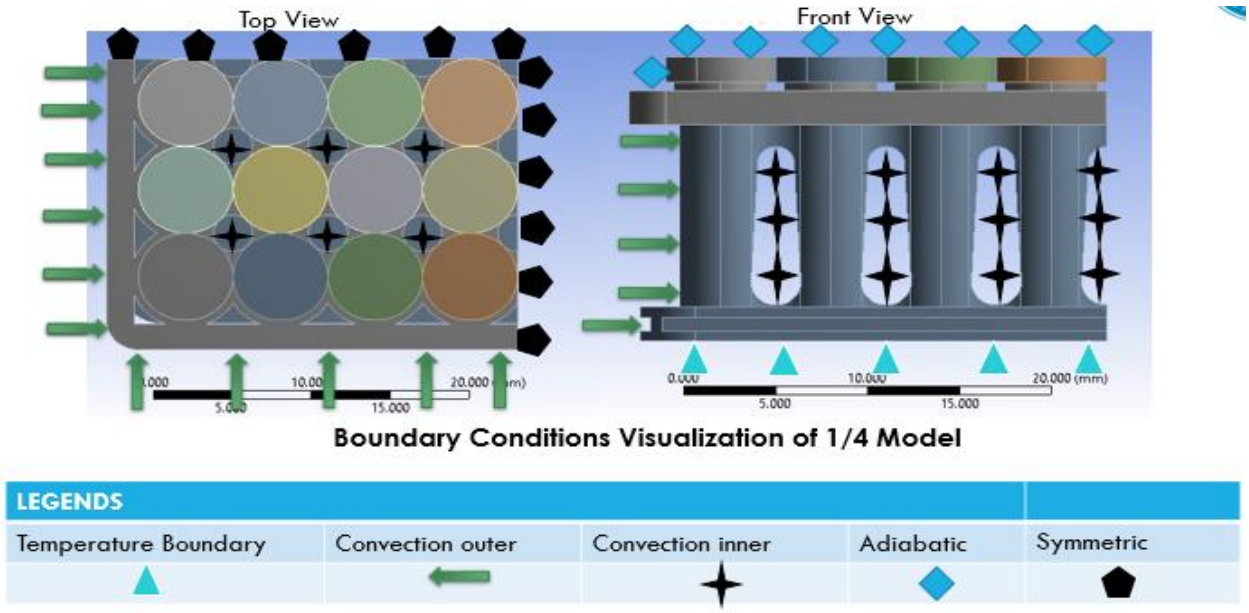

Figure 5.11: Boundary Conditions of transient thermal analysis

5.3.1. Thermal FEA to find thermal response of existing Technology

To have a clear idea we modelled the Bio-Rad CFX and Static Chamber device for having thermal response data. Bio-Rad CFX is a popular machine with fast thermal cycling capability in a typical multiwall qPCR machine using tubes and Static chamber PCR device which is same style of device as Bio-Rad but it is designed for more sample volumes. In the present work we designed analyzed the transient thermal PCR sample block and compared it with raouf et.al [1] and observed that design of current device is better in some ways than the device mentioned in [1].

First we list key properties of materials which we will encounter in design and modelling

Table 5.1: Thermal Properties of Selected Materials

Material	**Thermal conductivity** *W/mK*	**Specific Heat** *J /kg.˚C*	**Thermal diffusivity** $m^2/2$	**Co-efficient of thermal expansion** 10^{-6} *m/mK.*	**Specific Gravity**
Water	0.61	4182	0.143×10^{-6}	NA	1
Aluminum	205	897	8.418×10^{-5}	22.2	2.72
Copper	401	385	1.11×10^{-4}	16.6	8.79
COP 1420	0.15	1500	0.0986×10^{-6}	70	1.014
Polycarbonate	0.19	1170 - 1250	0.144×10^{-6}	70.2	1.2-1.22
Polypropylene	0.1-0.22	1920	0.096×10^{-6}	100 - 200	0.946

Table 5.2: Comparison of Thermal Properties

Material	Ratio of Thermal conductivity (k)	Ratio of Specific Heat	Ratio of Thermal diffusivity	Co-efficient of thermal expansion All vs Aluminum	Specific Gravity
Aluminum	336	0.21449	588.6	1	2.72
Copper	657	0.092061	776.223	0.747	8.79
COP 1420	0.245	0.358	0.6895	3.153	1.014
Polycarbonate	0.311475	0.29890	1.00699	3.162	1.2-1.22
Polypropylene	0.327	0.45911	0.67132	4.504-9	0.946

A Comparison of properties is given in Table 5.2. All materials are compared to Water except for coefficient of thermal expansion which is compared to Aluminum.

5.3.2. Bio-Rad CFX and Current study

The Bio-Rad low profile PCR simulation results are taken from the Raouf et.al [1]. The following procedure was adapted to get the required answers in current study after that the results are compared with Bio-Rad low profile PCR results.

1. The simulation is transient thermal only. We don't consider any material dimensional change.
2. Boundary Conditions: The base of the sample block were given the temperature boundary conditions. The plastic tube is in the Aluminum Sample block and thus we assume there is no air gap between the Sample block and the tube which is the best possible case. We also assume that the thermal block temperature at every position is equal at the boundary of the block. It is also assumed that thermal block thermal mass is much bigger than the PCR tube and we model the boundary as a constant temperature assuming that any amount of heat can be provided.
3. As the reaction occurs in a closed space, we considered very small convection coefficient from top of liquid to the surroundings and from the inner through, blind holes of Sample block as we calculated in previous chapter. However rouf et.al [1] did not considered this heat transfer convection effects. That was a valid assumption

due to low thermal conductivity of the tube and presence of large air gap inside the tube between the liquid surface and the cap

4. Natural convection of air from side walls of Sample block is very low and we considered the convection coefficient 3 Watt/m^2-k.
5. Natural convection is neglected inside the tube wall as well. Natural convection can speed up heat transfer.
6. Heating simulation is conducted from 55 to 95 ° C. initially the system is assumed to at initial temperature of 55 ° C. this models the condition that the cycler has been at 55 ° for a while so all elements reach 55 ° C.
7. The base of Sample block is given a boundary condition of temperature jump from 55 to 95 ° C. The temp is then held at 95 ° C. The speed of the system may be limited by ramp rate of the metal block but we are focusing on the liquid reservoir for comparison to other systems.
8. For cooling simulation similar procedure is adapter with temperature jump from 95 to 55 ° C.

The CFX-Bio Rad results presented below from the Raouf et.al [1].

Table 5.3: Time required to get uniform temperature fluid domain in plastic tubes

Operation	Volume	Time for liquid to equilibrate
Heating	25ul	~20 seconds
Heating	50ul	>13 seconds

To find out the effect of plastic tube on the heat transfer performance, we change the material of the tube to Aluminum. Following results are obtained.

Table 5.4: Time required to get uniform temperature fluid domain in Aluminum tubes

Operation	Volume	Time for liquid to equilibrate
Heating	25ul	~12 seconds
Heating	50ul	>23 seconds

The important point of Raouf et.al [1] are as follows.

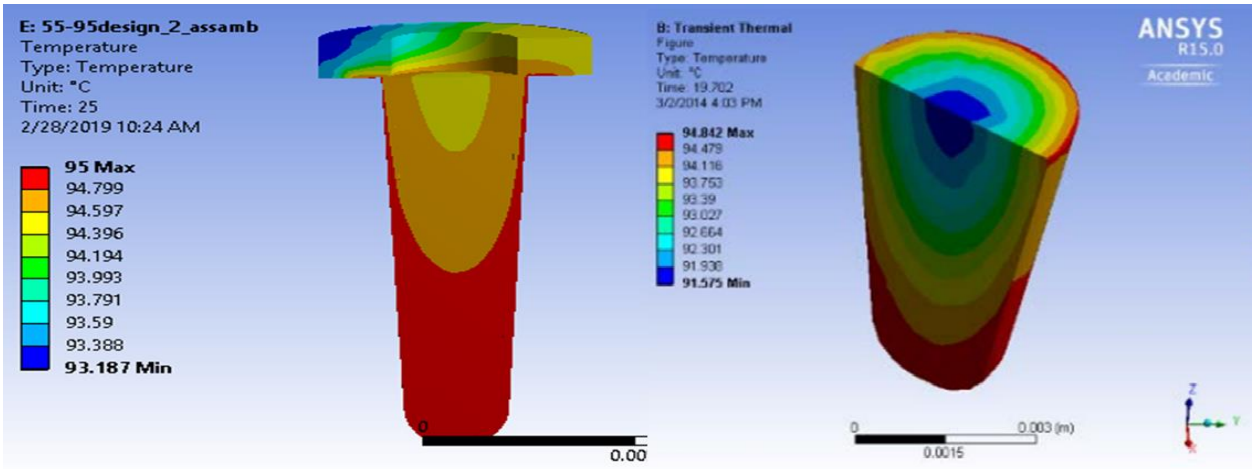

- The fluid in the tube takes considerable time to equilibrate even with metal walls. Thus this is not the optimum geometry if speed has to be increased.
- The polymer wall makes heat transfer considerably slower. Changing walls to metal can save significant time.

5.3.3. Results comparison of Bio-Rad CFX to current design

In Above picture the comparison of temperature uniformity is given for the current study and CFX Bio-Rad model given in [1]. The fluid domain of current model have more uniform temperature

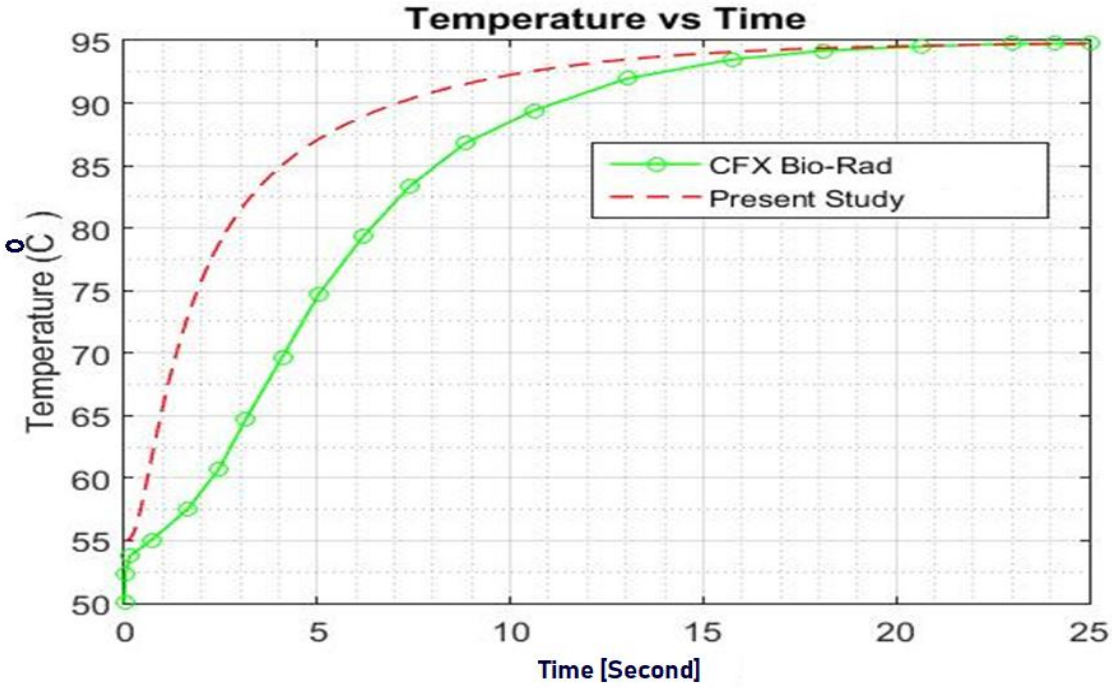

F

at 25 second. The temperature range of current study is 94.395 to 95 degree of fluid domain. Whenever the temperature range of [1] is 94.842 to 91.575 degrees.

The above graph shows the relation between temperature and time and it is observed that temperature variation in the current study is better than the [1] as it approaches to maximum temperature of 95 degrees in short time interval.

CHAPTER 6

RESULTS AND DISCUSSION

As the problem statement, here required to design a PCR DNA amplification device for the sample size 50microliter. For this in current work, initially different three dimensional model of Sample block are designed in Solidwork as required sample fluid. After that the sample block analyze in Steady state and Transient thermal. The temperature boundary conditions are applied at the base of well type Sample block, without any tube and fluid sample. After that polypropylene tube are modeled for 50 microliter sample fluid. The one cycle of temperature boundary condition is applied for DNA amplification are required temperature of thermal cycle to amplification.

6.1. Step to Design Sample Block

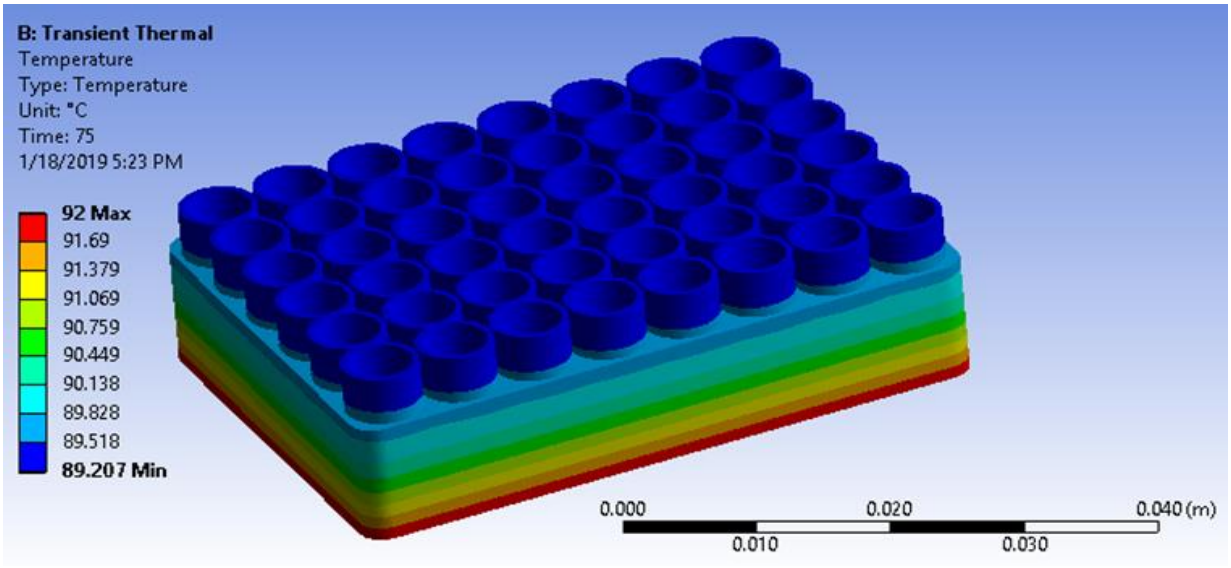

Figure 6.1: Transient Thermal analysis results of first step toward the design of Sample block

First we made three different designs using solid works. Each design contains a cell having storage capacity of 50 ml for fluid sample. The all three design were analyzed by applying transient boundary condition at base to observe the temperature response at the top surface of sample block. All the boundary conditions and temperature response are presented below in figure 6.4. Figure 6.1 to 6.3 show the contours of temperature of sample block. These contours show the variation of temperature at top surface and throughout the device. It is observed that at some places

temperature gradient is very low and thus negligible. At these places material is removed in the original design and a new optimum design is achieved with lower mass.

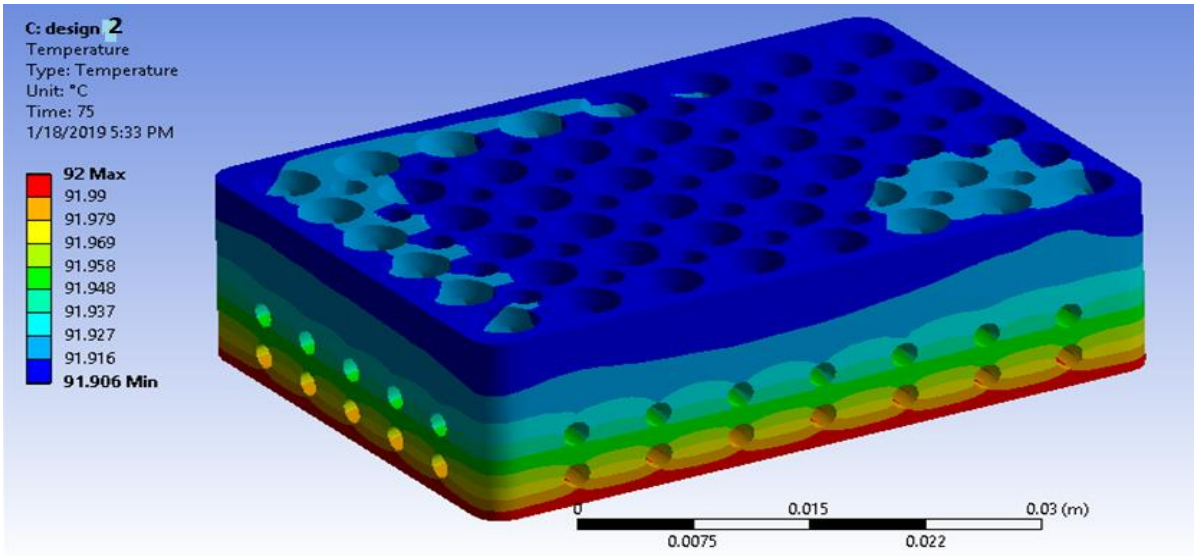

Figure 6.2: Transient thermal simulation contours of Temperature of step 2 toward design of Sample block

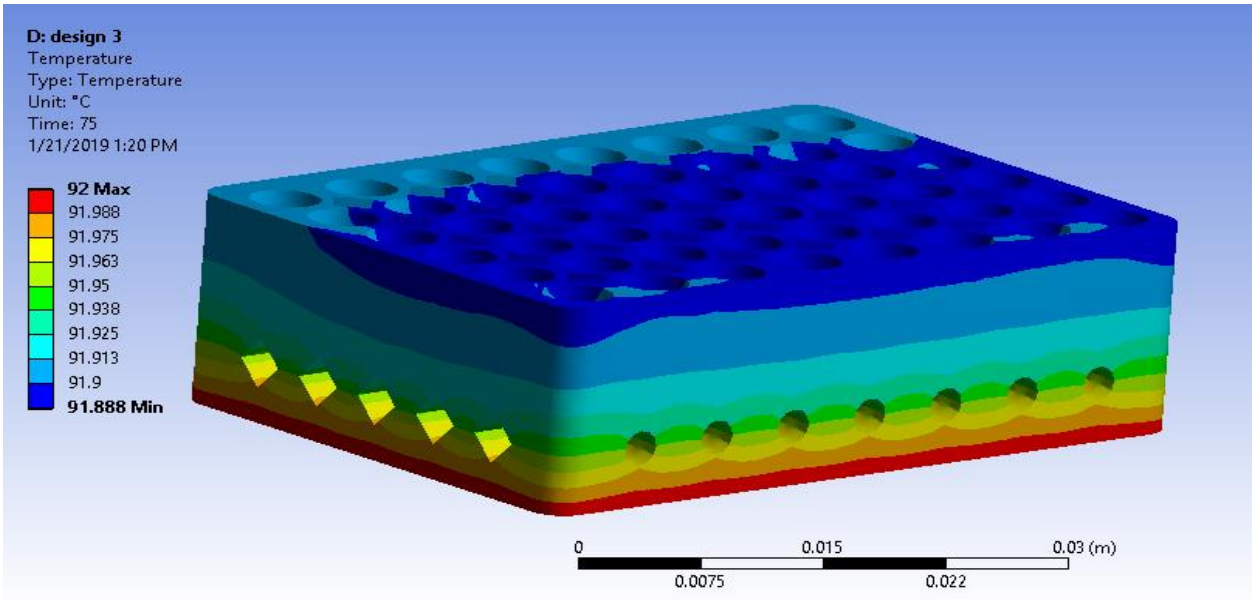

Figure 6.3: Transient thermal simulation contours of Temperature of step 3 toward design of Sample block

Table: mass of different design

Design	Mass (Gram)	Material	Volume (Cubic mm)
1	49.40	Aluminum	18297.25
2	47.28	Aluminum	17514
3	46.54	Aluminum	17238.4

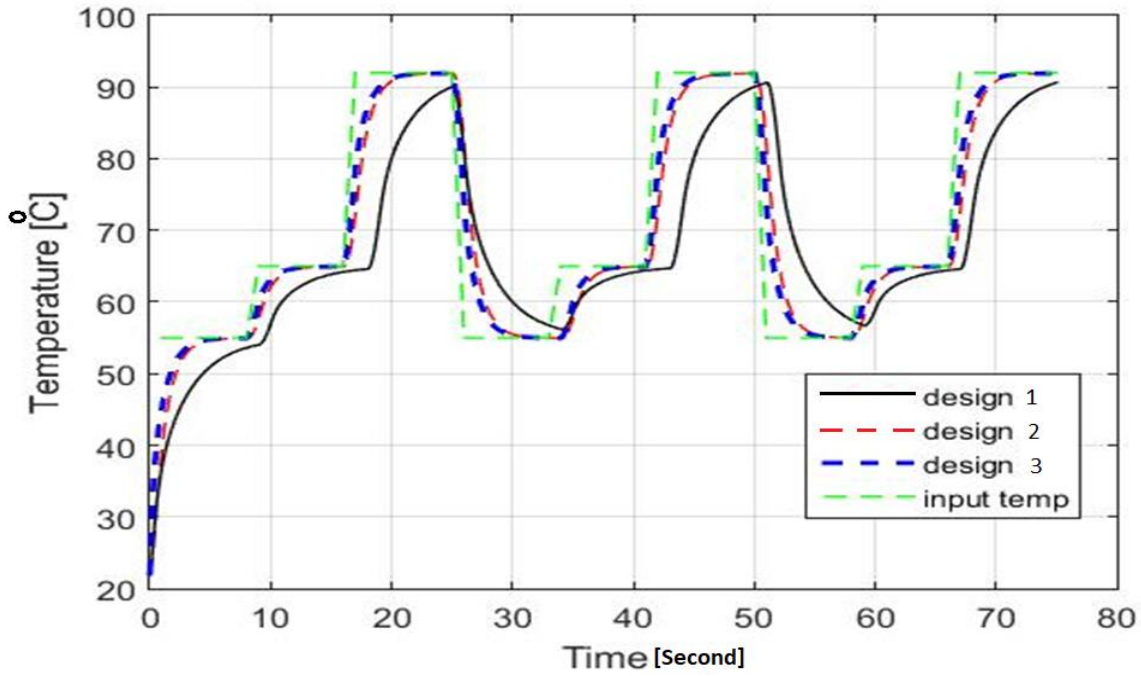

Figure 6.4: The results comparison of Temperature with time first 3 step

Three thermal cycles are applied to all designs and compared the temperature response at the top surface of device in the figure 6.4. it is obvious from figure 6.4 that response time of design 2 is higher than other two designs thus we choose this one and further analysis is performed on this design to get an optimum result.

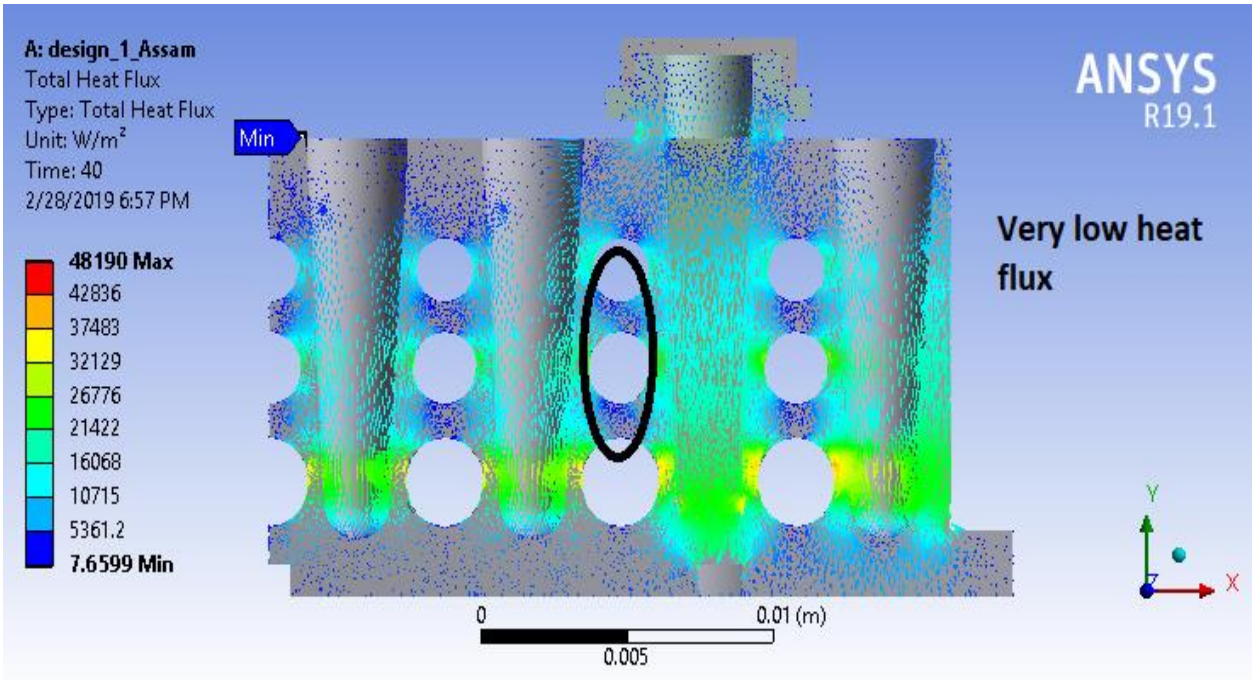

Figure 6.5: Sectioned view of heat flux contours

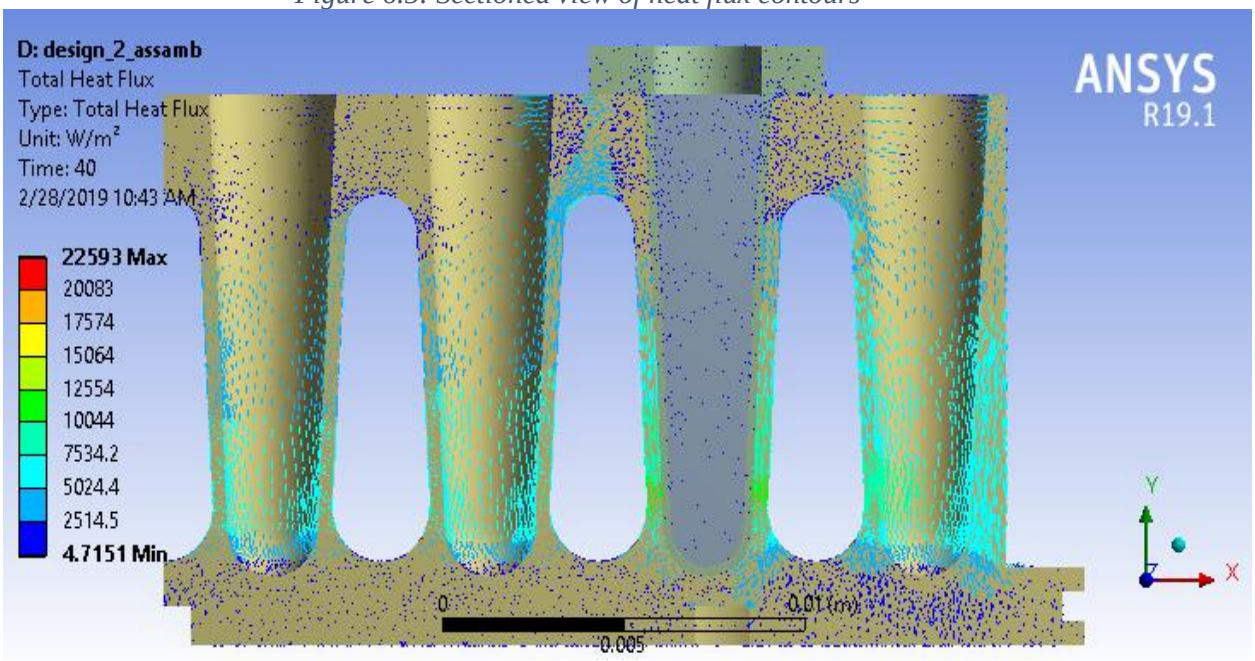

Figure 6.6: Sectioned view of heat flux contours

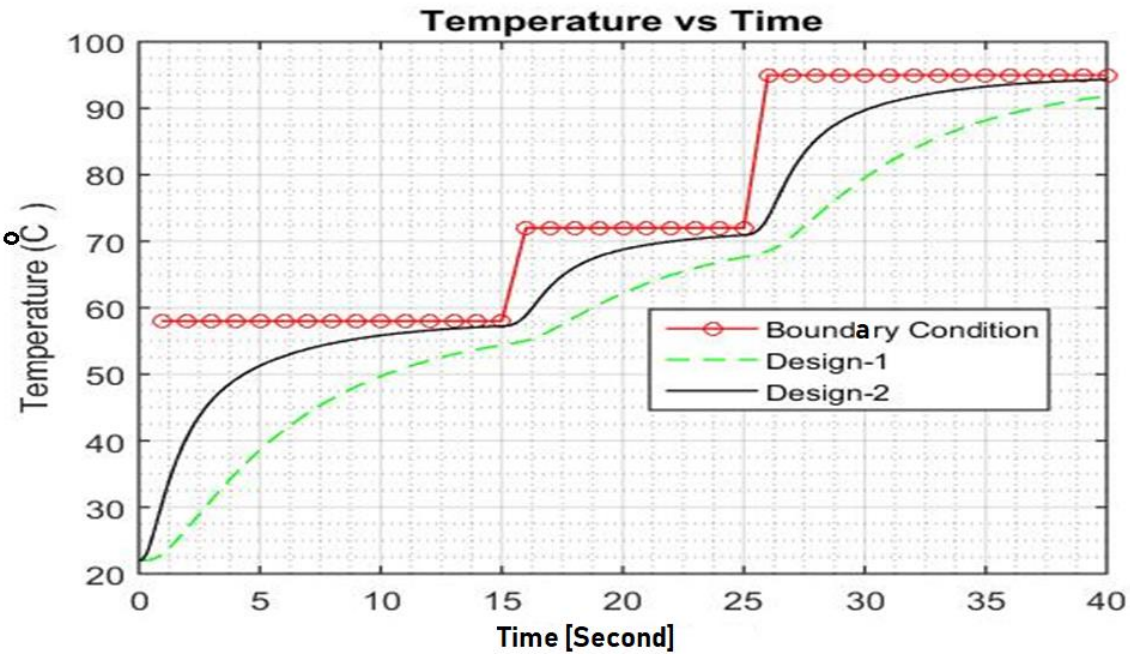

Figure 6.7: Variation of temperature with time of above discussed two assemblies

Design 2 is further improved using geometry features. In the figure 6.5 it is shown that in the sides of walls we made holes to reduce the thermal mass of sample block and performed simulation. It can be seen in figure 6.5 that the effect of heat flux on mass present between the holes is negligible. Then this design is again modified and the mass between the holes is removed completely making the shape of elliptical slot instead of holes and simulation is performed again. Figure 6.6 shows that this slot design is better than the presented in the figure 6.5. Temperature response time of the designs presented in figure 6.5 and 6.6 plotted in the figure 6.7. It is evident that design having lower mass have high temperature response that the other one presented in the figure 6.5.

6.2. Energy Consumption

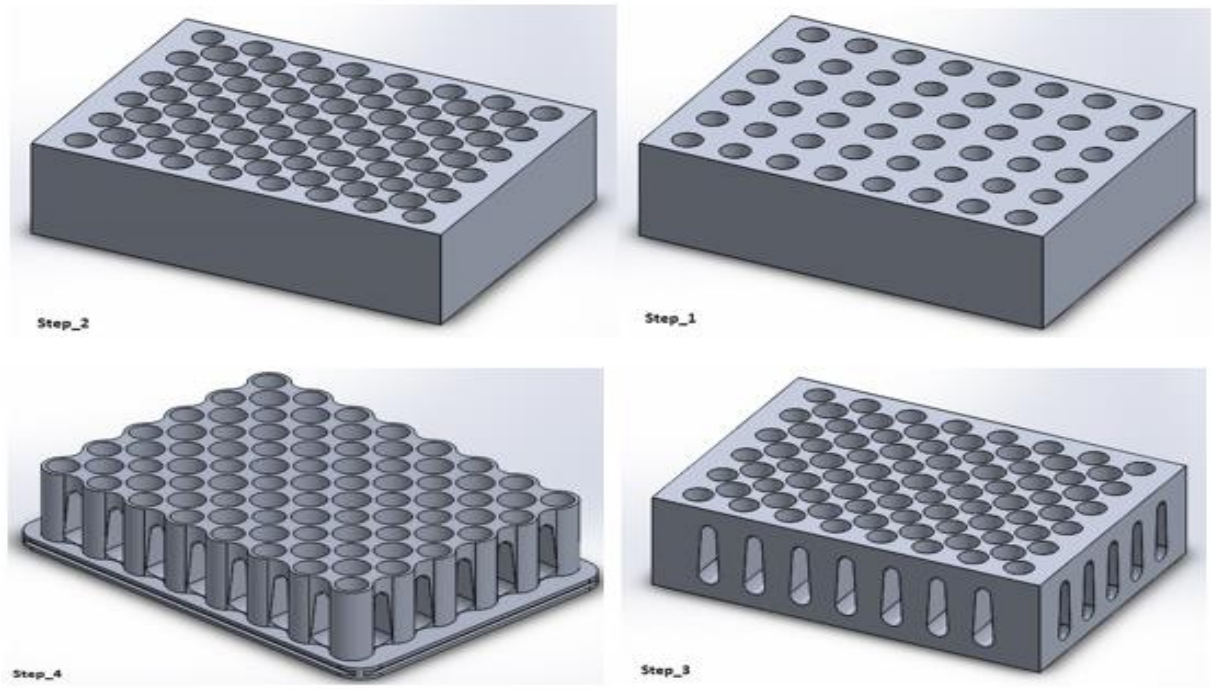

Figure 6.8: 4 steps of design of Sample block to analyze the effect of mass to energy consumption

Four steps of designing the sample block are shown in the figure 6.8. in each step mass is reduced using different geometrical shapes.

Step-1

A single rectangular block is shown with wells only having mass of 61.27 g.

Step-2

The material between the wells is removed using blind holes of 4mm diameter. Now the mass is reduce to 46.5 g.

Step-3

In the further design consideration extra material from sides is removed by making elliptical slots. Now mass became 31.91 g.

Step-4

In this final step material from side walls is removed to for better appearance of device. And the final mass of block is 23.5 g that is optimum for current design. Material used is aluminum that is used mostly in these devices.

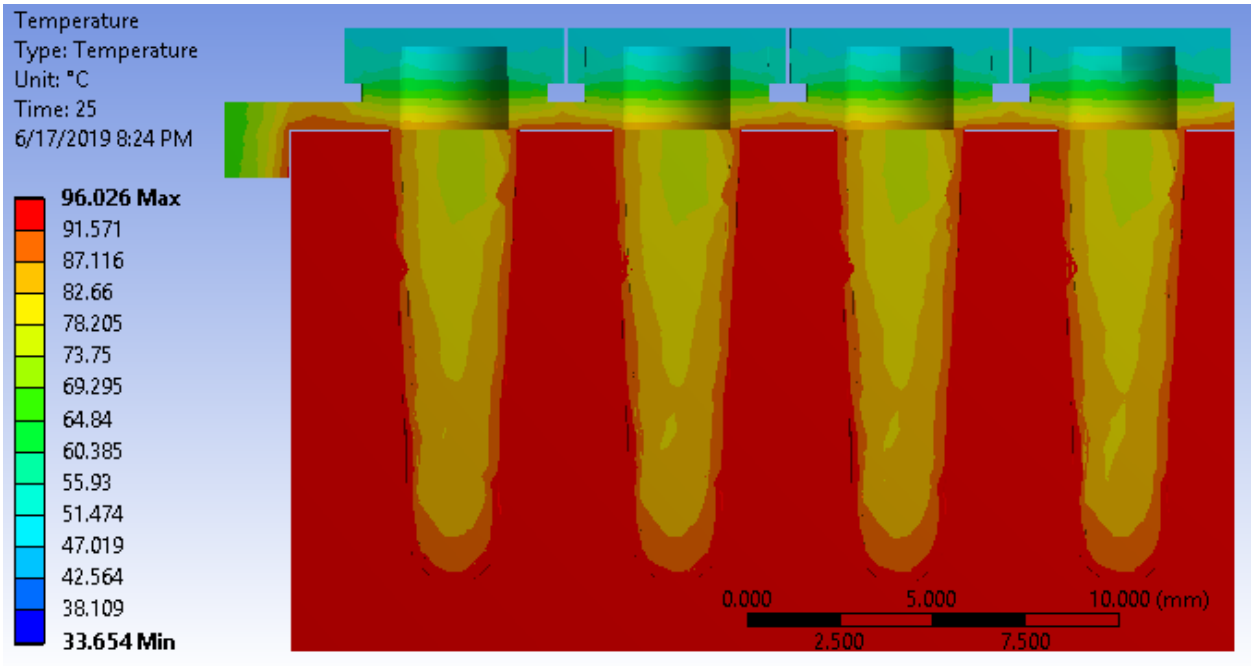

Figure 6.9: Temperature contours of step 1 PCR device assembly at 50 watt input boundary

Plastic tubes are placed in the wells of these devices and fluid sample is kept in these tubes and glass caps are placed above the tubes to stop the evaporation of fluid sample. Then a heat flux of 50 watt is given to all the devices at base. Then temperature response of all the device at the heat flux of 50 watt is shown in the figures from 6.9 to 6.12. It shown clearly from the section views of devices that the device having minimum thermal mass gives the highest temperature response. It can be seen that by removing the thermal mass energy requirement is reduced for designing the portable devices.

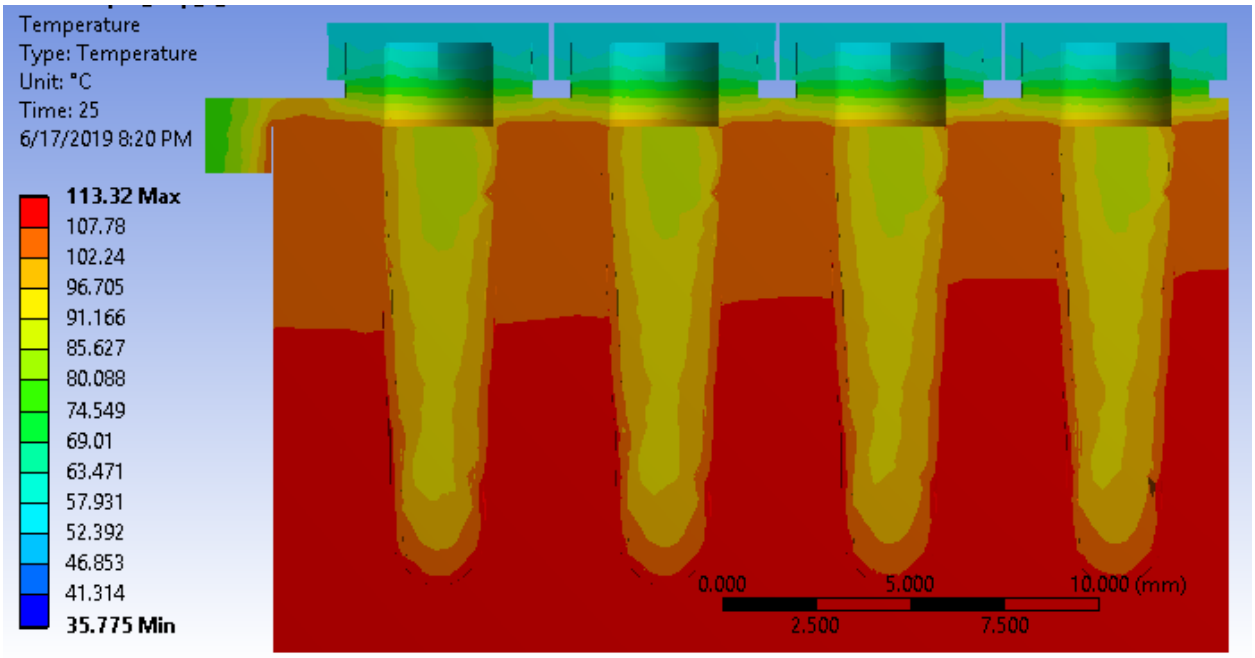

Figure 6.10: Temperature contours of step 2 PCR device assembly

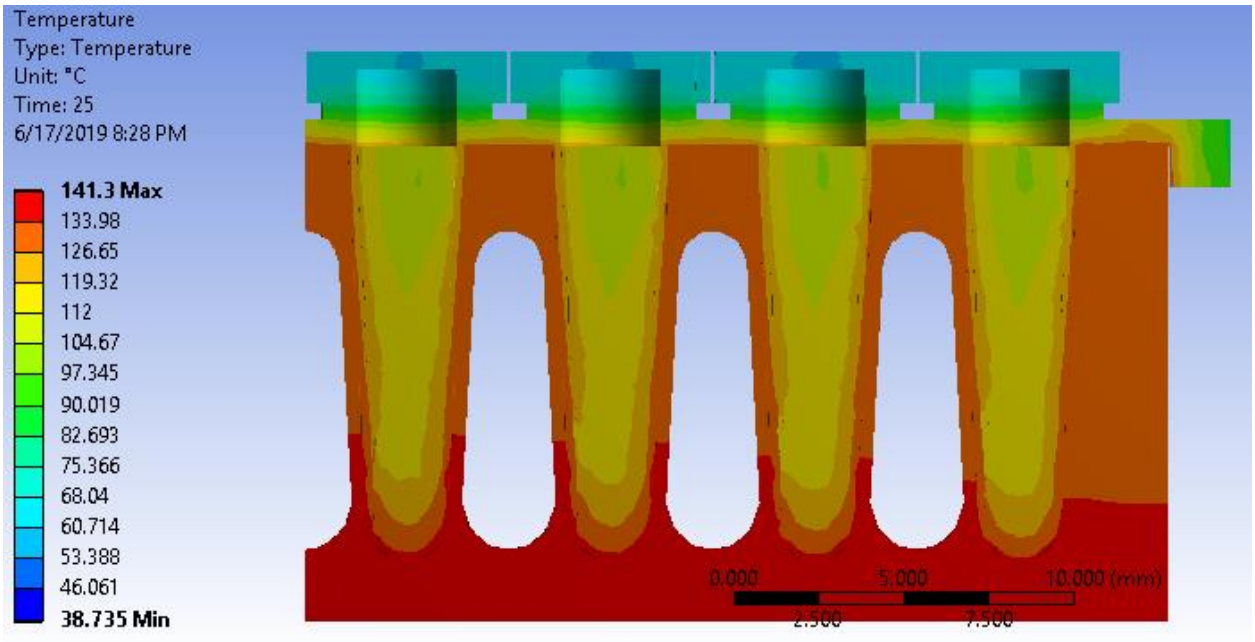

Figure 6.11: Temperature contours of step 3 PCR device assembly

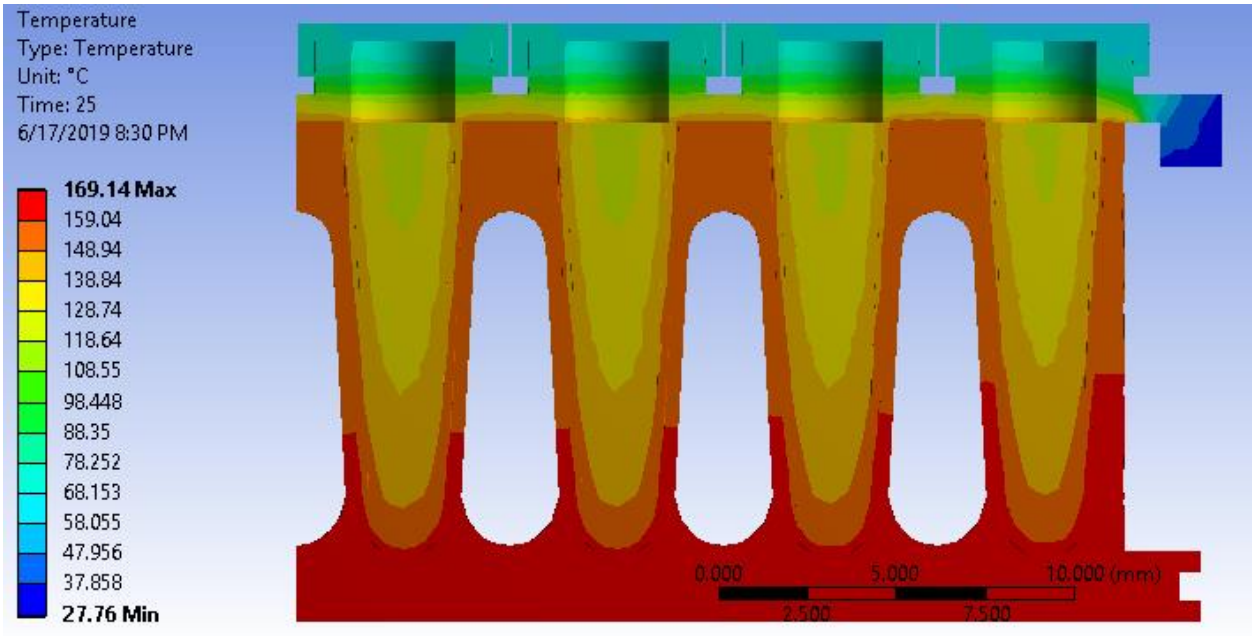

Figure 6.12: Temperature contours of step 4 PCR device assembly

Table 6.2: Effect of Sample block mass on applied energy

Steps	Mass of Sample Block (gram)	Maximum temperature (ºC)	Input power (Watt)	Energy saving
1	61.27	96.061	50	0%
2	46.5	96.542	40.5	19%
3	31.91	96.643	30.8	38.4%
4	23.5	96.348	24.75	50.5%

Four different sample blocks are compared in the table above. We required a temperature of 96 to 97 degrees. First a heat flux of 50 watts is given to all the devices and response is recorded. Then an optimum design is selected from above mentioned designs that is having a mass of 23.5 g. after that we calculated the energy required to gain our desired temperature value. It is shown that about 50.5% energy is saved as compared to the design having thermal mass of 63.21 g.

6.3 Sample Block material

The intensive interplay of engineering and materials science has always been an important driving force in the rapid evolution of microfluidic technologies and their strikingly wide range of applications. To date, numerous materials, including silicon, quartz/fused silica, glass, ceramics,

polymers, copper, silver and aluminum have been used in fabricating microfluidic devices bearing diverse functionalities. In general, a microfluidic device can be built by first fabricating (by dry or wet etching, mechanical machining, molding, or casting) but the sample block of microfluidic device can manufacture by machining only. The general material for sample block are copper, silver and aluminum used in literature but the silver is expensive that is why this is neglected to made lowest price device.

The below graph show the temperature response of copper and aluminum sample block. The uniform temperature is applied at the base of the sample block for 25 second and temperature sensor is placed at the top of fluid sample. The copper sample block show the quick response of applied temperature.

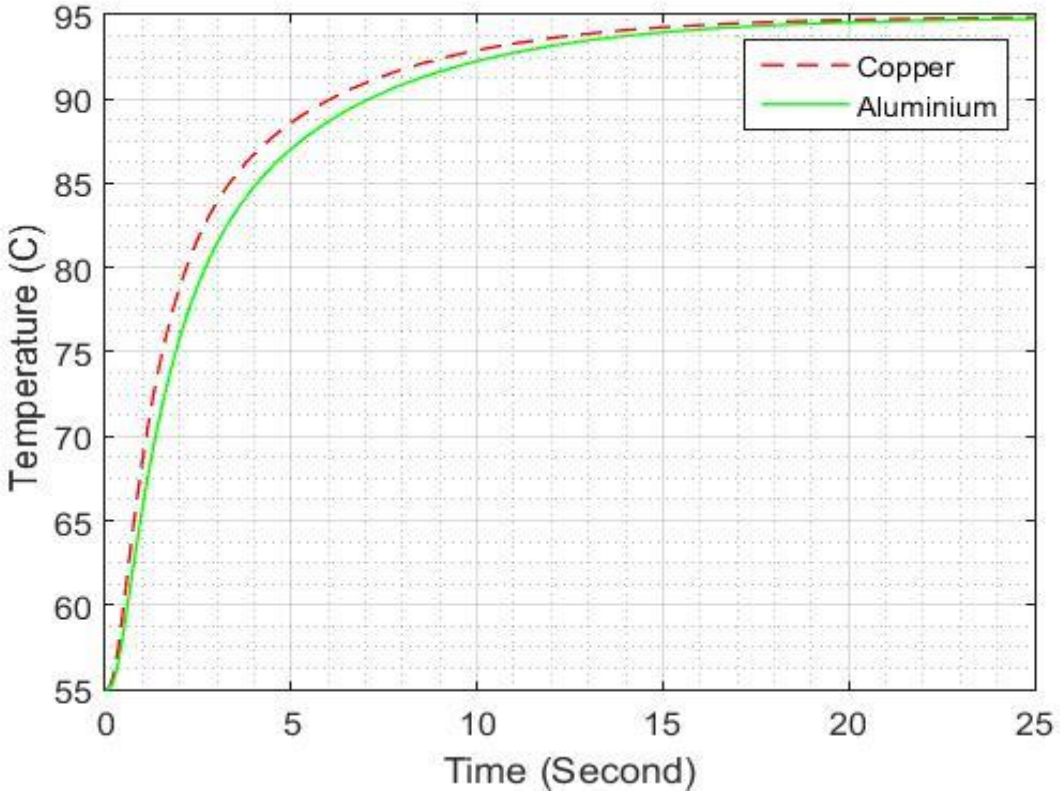

Figure 6.13: The temperature response of different material sample block

6.4. Thermo Electric Heating and Cooling Element (Peltier)

In the above presented analysis temperature and heat flux boundary conditions are applied to heat the sample block. But in real time application we need both cooling and heating device that can reduce the PCR cycle time. First step of PCR is denaturation in which temperature requirement is from 92 to 97 degrees. Second step of PCR is primer annealing in which temperature is reduced between 55 to 60 degrees. Thus here we need a device that can perform both heating and cooling operations when required. So a Peltier is selected for this heating and cooling purpose. It consists of number of thermoelectric cells that are placed in the series. Numbers of cells in a Peltier depends upon the temperature requirements. In the current study a Peltier consists of 70 cells is used. The figure 6.14 shown the basic working of device.

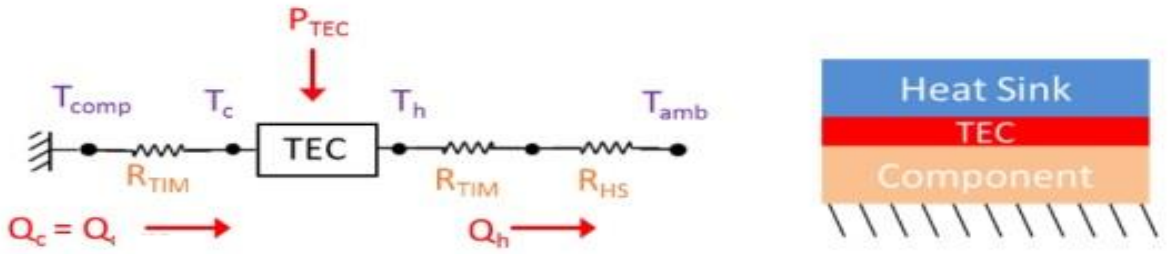

Figure 6.14: working of thermoelectric component

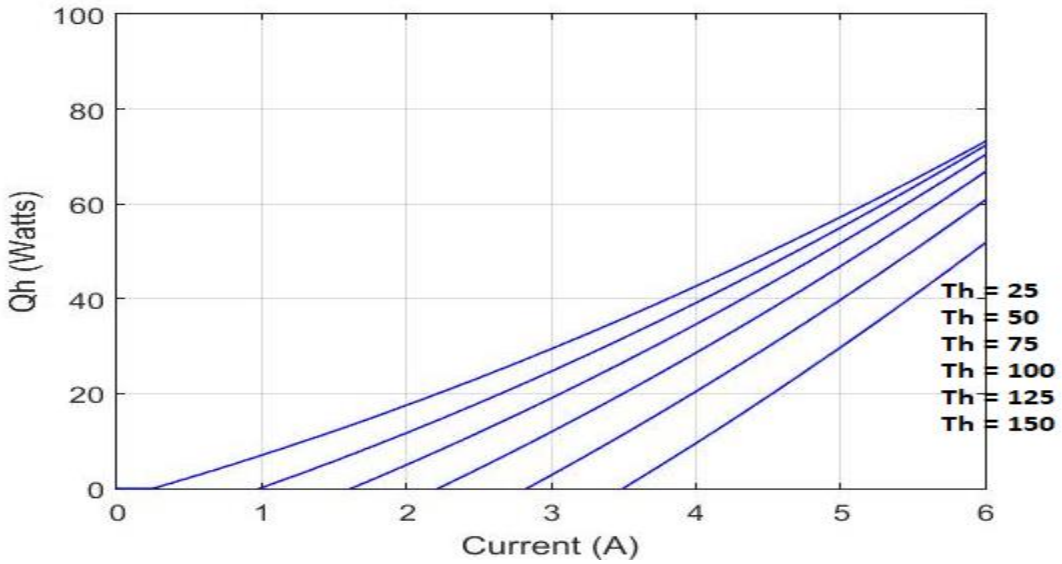

Figure 6.15: Q_h to applied current graph at different high temperature

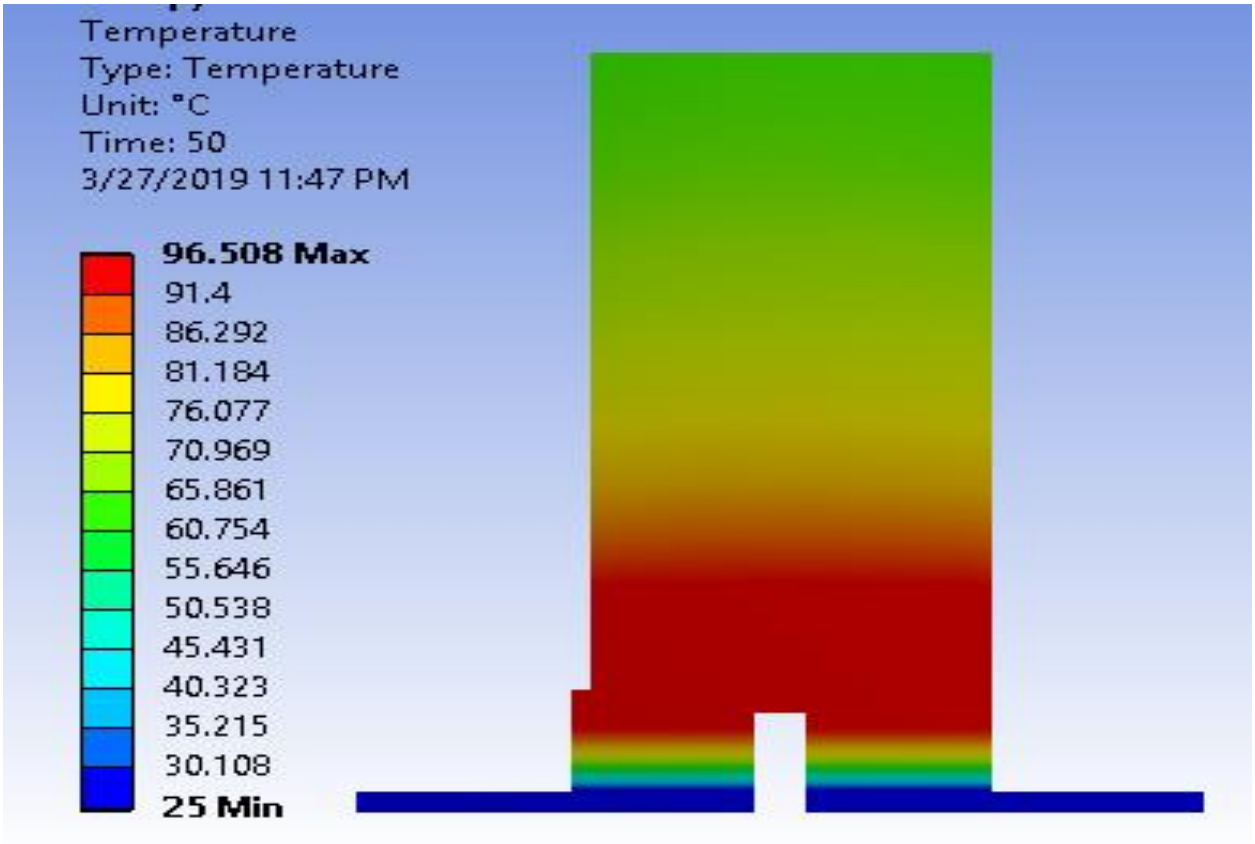

Figure 6.16: temperature contours with single cell thermoelectric module

The figure 6.16 shows the single cell of Peltier element with the unit cell of device. As the current passes from the Peltier element it heats the one side and cools the other. The unit cell of device is placed on hot side of Peltier, the hot side showing the temperature is 96.5 degree. The current is applied at copper element of Peltier and other side of cell is grounded. The convection boundary condition is applied at the side of unit cell of device with convection heat transfer coefficient 3 $W/m^2.K$. The opposite side of the Peltier is cooling side.

After analysis of Peltier single cell effect, we analyzed the device by applying the symmetry in Thermal Electric module of ANSYS. The temperature contours of PCR device with thermoelectric module heating are shown in figure 6.17. The 4.5 Ampere current is applied at positive terminal and negative terminal is grounded whenever 6 volt battery is required for this Peltier. If we reverse the current direction it will cool the top surface and heat generated on base of Peltier the where need to place the fins to dissipate this generated heat to atmosphere to get maximum cooling.

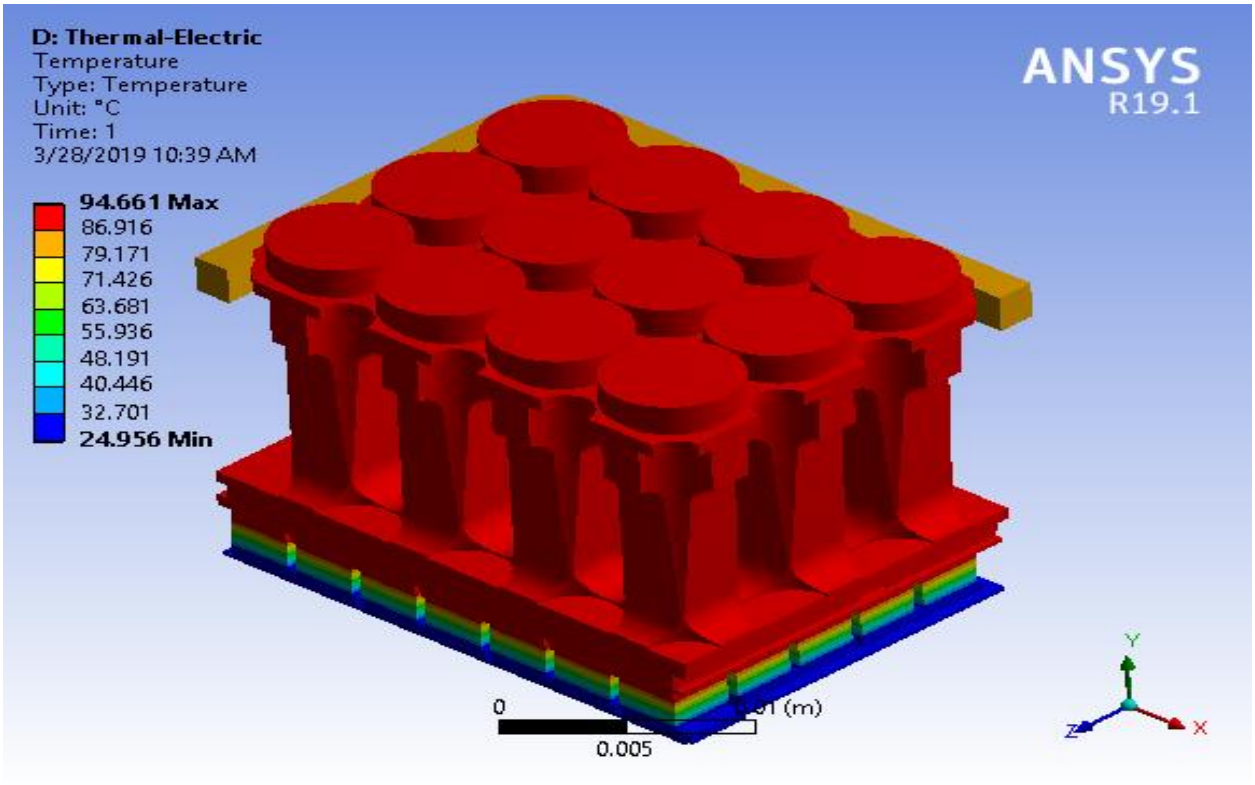

Figure 6.17: temperature contours of one fourth device with heating by Peltier

6.5. Final Design and Drawings

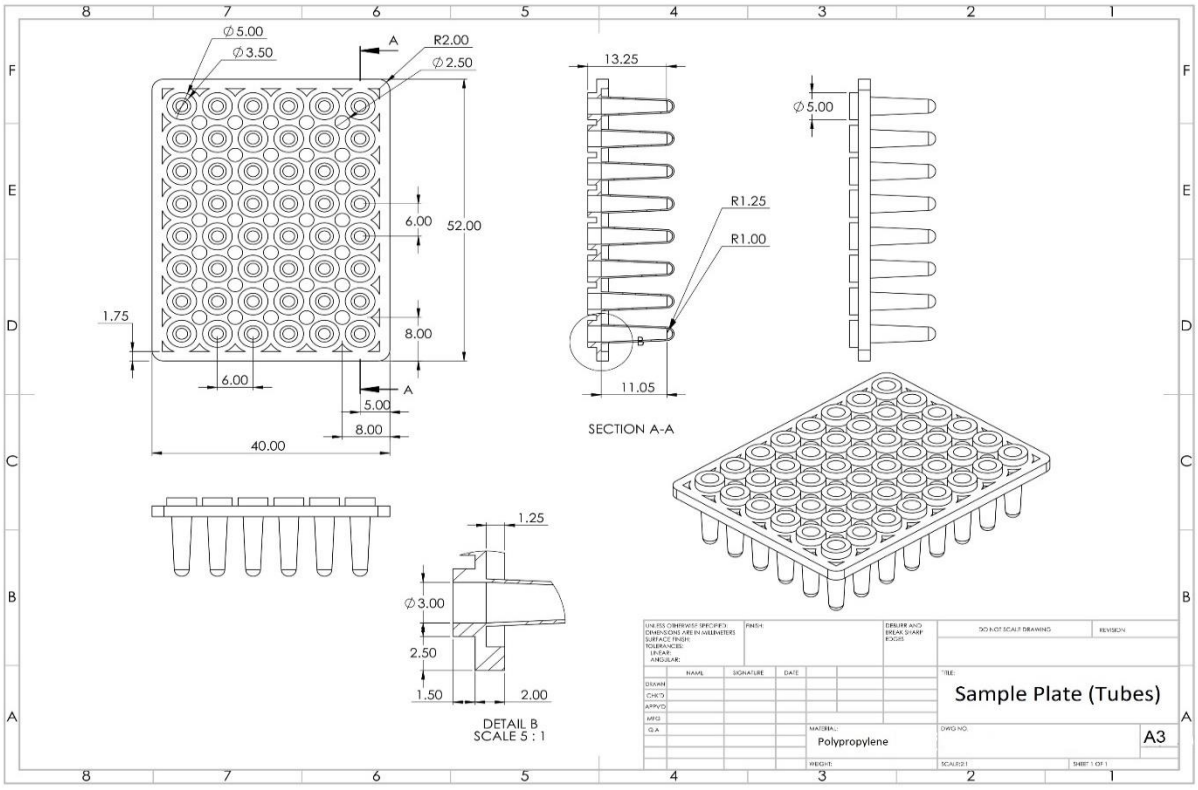

Figure 6.14: The Polypropylene tubes plate

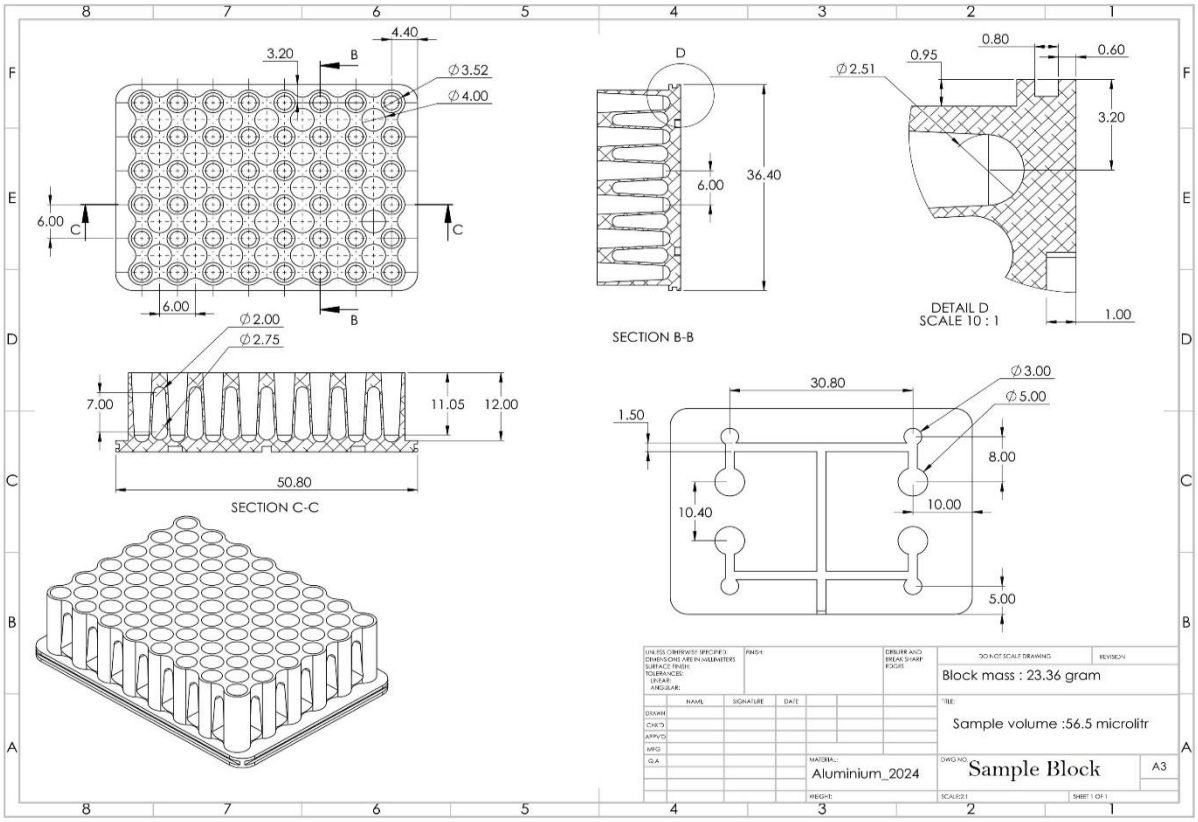

Figure 6.15: Sample Block

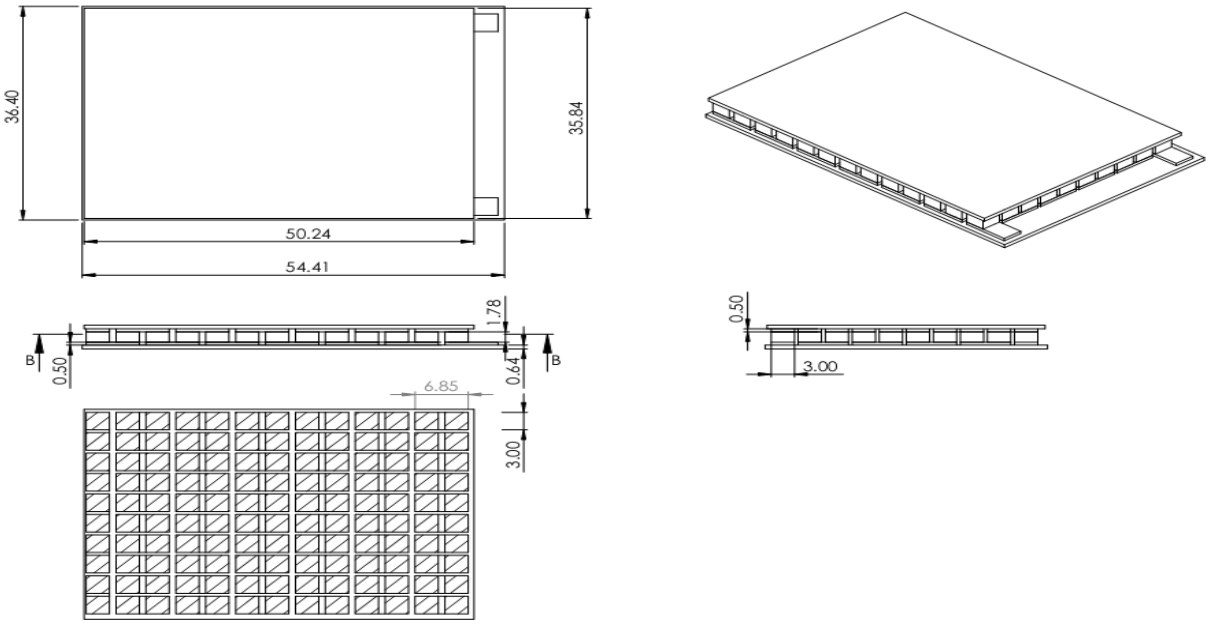

Figure 6.16: Thermoelectric Component (TEC)

6.6. Conclusion

The devices used for polymerase chain reaction (PCR) available in the market at commercial level are expensive and can handle the sample size of about 30 ml. in the present work these two parameters are considered and a PCR device is designed. To achieve the better performance and research objective different designs are made and simulated in Ansys to check their performance and compactness. Initially 3 designs are made and only sample block are analyzed. Then we choose one from these on the basis of temperature response time of sample block. After that the chosen design is further analyzed and modified in terms of thermal mass and energy requirements. Heat flux is used for heating the sample block. Temperature uniformity and response time are achieved for final design. Then thermal mass of sample block is reduced in different ways to check the effect on the thermal response. First 48 wells were generated in the sample block. Then tubes are placed in these holes having glass caps. A heat flux of 50 watt applied to it and analyzed the temperature response. This was near to our required temperature that is 97 degrees. After this thermal mass is reduced by making blind holes on the top surface of sample block to check the effect on new sample block with lower mass. It is observed that from removing thermal mass same temperature response is achieved with low energy and about 29% of energy is saved. From the temperature contours some part is observed again where the temperature affects are negligible. In the final design these areas are removed by making elliptical slots in both sides of sample block and analysis is performed. Material present at sides is also removed in the final design for better appearance but left a small rib at the bottom side to clamp the device easily. In this final design about 50.5 % energy is saved as compared to initial design.

Initially a heat source of 50 watts was applied at the base of sample block using the heat flux boundary conditions. But in the real applications this heat source difficult to apply. So, for the heating and cooling purpose a Peltier is used. Peltier is a well-known heating and cooling device. But in the current work Peltier is used only for heating the sample block. After analysis of Peltier single cell effect, we analyzed the device by applying the symmetry in Thermal Electric module of ANSYS. The 4.5 Ampere current is applied at positive terminal and negative terminal is grounded whenever 6 volt battery is required for this Peltier. If we reverse the current direction it will cool the top surface and heat generated on base of Peltier the where need to place the fins to dissipate this generated heat to atmosphere to get maximum cooling.

In the end lowest possible mass, temperature uniformity of fluid sample and a good temperature response rate is achieved for the best possible working of device.

In the present work Peltier is used only for the heating purpose. In the future it can be used for reducing the temperature of device after denaturation. Heat generated on the other side of device during the cooling of device can go dissipate to sink. This sink can also be designed in future. Another way of cooling may be by passing the air through the elliptical slots. The air would remove the heat by convective heat transfer. The results of current work can also be validated through experimental work by manufacturing the device.

References:

1. Imran Raouf Malik PhD Theisis “Point of Care Molecular Diagnostics for Humanity”

2. K. Mullis, F. Faloona, S. Scharf, R. Saiki, G. Hom, H. Erlich, “Specific enzymatic amplification of DNA in vitro: the polymerase chain reaction,” Cold Spring Harbor Symp Quant Biol, vol. 51, pp. 263–284, 1986.

3. Y. Zhang, P. Ozdemir, “Microfluidic DNA amplification review,” Anal Chim Acta, vol. 638, pp. 115–125, 2009.

4. C. Gartner, R. Klemm, H. Becker, “Methods and instruments for continuous-flow PCR on a chip,” in: Proc. Microfluidics, BioMEMS and Medical Microsystems V San Jose, SPIE, vol. 6465, 2007, pp. 6465502-1–6465502-8.

5. H. Nakano, K. Matsuda, M. Yohda, T. Nagamune, I. Endo, T. Yamane, “High-speed polymerase chain-reaction in constant flow,” Biosci. Biotechnol. Biochem., vol. 58, pp. 349– 352, 1994.

6. N. A. Friedman, D. R. Meldrum, “Capillary tube resistive thermal cycling,” Anal. Chem., vol. 70 pp. 2997-3002, 1998.

7. J. Chiou, P. Matsudaira, A. Sonin, D. Ehrlich, “A Closed-Cycle Capillary Polymerase Chain Reaction Machine,” Anal. Chem., vol. 73, pp. 2018-2021, 2001.

8. H. Tachibanaa, M. Saitoa, K. Tsujib, K. Yamanakaa, L. Q. Hoaa, E. Tamiyaaa, “Selfpropelled continuous-flow PCR in capillary-driven microfluidic device: Microfluidic behavior and DNA amplification,” Sensors and Actuators B, vol. 206, pp. 303–310, 2015.

9. M. U. Kopp, A. J. D. Mello, A. Manz, “Chemical amplification: continuous-flow PCR on a chip,” Science, vol. 280, pp. 1046–1048, 1998.

10. I. Schneegaß, R. Brautigam, J. M. Kohler, “Miniaturized flow-through PCR with different template types in a silicon chip thermocycler,” Lab Chip, vol. 1, pp. 42–49, 2001.

11. I. Pjescic, C. Tranter, P. L. Hindmarsh, N. D. Crews, “Glass-composite prototyping for flow PCR with in situ DNA analysis,” Biomed. Microdevices, vol. 12, pp. 333-343, 2010.

12. L. Jiang, M. Mancuso, Z. Lu, G. Akar, E. Cesarman, D. Erickson, “Solar thermal polymerase chain reaction for smartphone-assisted molecular diagnostics,” Sci. Rep., vol. 4:4137, 2014.

13. N. Park, S. Kim, J. H. Hahn, “Cylindrical compact thermal-cycling device for continuous flow polymerase chain reaction,” Anal. Chem., vol. 75(21), pp. 6029−6033, 2003.

14. M. Hashimoto, F. Barany, F. Xu, S. A. Soper, “Serial processing of biological reactions using flow-through microfluidic devices: Coupled PCR/LDR for the detection of low abundant DNA point mutations,” Analyst, vol. 132, pp. 913-921, 2007.

15. B. W. Shu, C. S. Zhang, D. Xing, “Segmented continuous-flow multiplex polymerase chain reaction microfluidics for high-throughput and rapid foodborne pathogen detection,” Anal. Chim. Acta., vol. 826, pp. 51−60, 2014.

16. M. Hashimoto, P. C. Chen, M. W. Mitchell, D. E. Nikitopoulos, S. A. Soper, M. C. Murphy, "Rapid PCR in a continuous flow device," Lab Chip, vol. 4, pp. 638-645, 2004.

17. J. West, B. Karamata, B. Lillis, J. P. Gleeson, J. Alderman, J. K. Collins, W. Lane, A. Mathewson, H. Berney, “Application of magneto hydrodynamic actuation to continuous flow chemistry,” Lab Chip, vol. 2, pp. 224–230, 2002.

18. K. Mullis, F. Faloona, S. Scharf, R. Saiki, G. Horn and H. Erlich, Cold Spring Harbor Symp. Quant. Biol., 1986, 51, 263 –273.

19. R. Saiki, D. Gelfand, S. Stoffel, S. Scharf, R. Higuchi, G. Horn, K. Mullis and H. Erlich,Science, 1988, 239 , 487–491.

20. H. M. Temin,Virology, 1963, 20, 577–582.

21. F. F. Chehab and Y. W. Kan, Proc. Natl. Acad. Sci. U. S. A., 1989, 86, 9178 – 9182.

22. F. Osman, E. Hodzic, A. Omanska-Klusek, T. Olineka and A. Rowhan i,J. Virol. Methods, 2013, 194, 138–145.

23. Y. Kim, Y. Choi, B.-Y. Jeon, H. Jin, S.-N. Cho and H. Lee, Yonsei Med. J., 2013, 54, 1220 –1226.

24. J. F. Mehrabadi, P. Morsali, H. R. Nejad and A. A. Imani Fooladi, J. Infect. Public Health, 2012, 5, 263–267.

25. A. Abd-Elmagid, P. A. Garrido, R. Hunger, J. L. Lyles, M. A. Mansfield, B. K. Gugino, D. L. Smith, H. A. Melouk and C. D. Garzon, J. Microbiol. Methods, 2013, 92, 293–300.

26. M. Safdar and M. F. Abas ıyan ık, Appl. Biochem. Biotechnology. 2013, 171, 1855 – 1864.

27. A. Manz, N. Graber and H. M. Widmer, Sens. Actuators, B, 1990, 1, 244–248.

28. P. Wilding, M. A. Shoffner and L. J. Kricka, Clin. Chem., 1994, 40, 1815 – 1818.

29. M. A. Northrup, C. Gonzalez, S. Lehew and R. Hills, Micro Total Analysis Systems: Proceedings of the μ TAS '94 Workshop, Springer, 1995, p. 139.

30. J. Cheng, M. A. Shoffner, K. R. Mitchelson, L. J. Kricka and P. Wilding, J. Chromatogr. A, 1996, 732, 151–158.

31. M. U. Kopp, A. J. d. Mello and A. Manz, Science, 1998, 280, 1046–1048.

32. P. A. Auroux, Y. Koc, A. deMello, A. Manz and P. J. R. Day, Lab Chip , 2004, 4, 534–546.

33. L. Chen, A. Manz and P. J. R. Day, Lab Chip, 2007, 7 ,1413–1423

34. D. Moschou, N. Vourdas, G. Kokkoris, G. Papadakis, J.Parthenio s, S. Chatzandroulis and A. Tserepi, Sens. Actuato rs, B, 2014, 199 , 470–478.

35. M. L. Ha and N. Y. Lee,Food Control , 2015, 57, 238–245.

36. J. Wu, W. Guo, C. Wang, K. Yu, Y. Ma, T. Chen and Y. Li, Cell Biochem. Biophys. , 2015, 72, 605– 610.

37. A. Harandi and T. Farquhar, J. Micromech. Microeng. 2014, 24, 115009.

38. H. Tachibana, M. Saito, K. Tsuji, K. Yamanaka, L. Q. Hoa and E. Tamiya, Sens. Actuators, B , 2015, 206 , 303–310.

39. J. J. Chen, M. H. Liao, K. T. Li and C. M. Shen, Biomicrofluidic s, 2015, 9, 014107.

40. W. Wu and N. Y. Lee, Anal. Bioanal. Chem., 2011, 400, 2053–2060.

41. Y. Schaerli, R. C. Wootton, T. Robinson, V. Stein, C.Dunsby, M. A. A. Neil, P. M. W. French, A. J. deMello, C. Abell and F. Hollfelder, Anal. Chem., 2009, 81, 302–306.

42. L. Jiang, M. Mancuso, Z. Lu, G. Akar, E. Cesarman and D. Erickson,Sci. Rep. , 2014, 4 , 4137.

43. R. Snodgrass, A. Gardner, L. Jiang, C. Fu, E. Cesarman and D. Erickson, PLoS One, 2016, 11, e0147636.

44. Y. Li, C. Zhang and D. Xing, Microfluid. Nanofluid. 2010, 10, 367–380.

45. B. Miao, N. Peng, L. Li, Z. Li, F. Hu, Z. Zhang and C. Wang, Sensors, 2015, 15, 27954

46. C. Zhang, H. Wang and D. Xing, Biomed. Microdevices, 2011, 13, 885–897.

47. A. G. Sciancalep ore, A. Polini , E. M ele, S. Girardo, R. Cingolani and D . P isignano , Bio sens. Bio electron. 2011, 26, 2711–2715.

48. Z. Li, T.-Y. Ho and K. Chakrabarty, ACM Transactions on Design Automation of Electronic Systems, 2016, 21, 1– 27.

49. R. Prakash, K. Pabbaraju, S. Wong, A. Wong, R. Tellier and K. Kaler, Micromachines, 2015, 6, 63.

50. M. J. Jebrail, R. F. Renzi, A. Sinha, J. Van De Vreugde, C. Gondhalekar, C. Ambriz, R. J. Meagher and S. S. Branda, Lab Chip , 2015, 15, 151–158.

51. Y.-F. Hsieh, E. Yonezawa, L.-S. Kuo, S.-H. Yeh, P.-J. Chen and P.-H. Chen,Appl. Phys. Lett. , 2013, 102, 173701.

52. K. Chan, P.-Y. Wong, P. Yu, J. Hardick, K.-Y. Wong, S. A.Wilson, T. Wu, Z. Hui, C. Gaydos and S. S. Wong,PLoS One, 2016, 11, e0149150.

53. J. S. Farrar and C. T. Wittwer, Clin. Chem., 2015, 61,145 – 153.

54. Y. Ouyang, G. R. M. Duarte, B. L. Poe, P. S. Riehl, F. M. dos Santos, C. C. G. Martin-Didonet, E. Carrilho and J. P.Landers, Anal. Chim. Acta, 2015, 901, 59 –67.

55. A. M. Schrell and M. G. Roper, Analyst, 2014, 139, 2695–2701.

56. N. Pak, D. C. Saunders, C. R. Phaneuf and C. R. Forest, Biomed. Microdevices, 2012, 14, 427– 433.

57. Ilic, A. Manz and P. Neuzil, Lab Chip ,2016, 16, 586–592.

58. C. D. Ahrberg, A. Manz and P. Neužil, Anal. Chem., 2016, 88, 4803 –4807.

59. C. D. Ahrberg, A. Manz and P. Neuzil, Sci. Rep. , 2015, 5 ,11479.

60. E. K. Wheeler, C. A. Hara, J. Frank, J. Deotte, S. B. Hall, W. Benett, C. Spadaccini and N. R. Beer, Analyst, 2011, 136 ,3707–3712.

61. T. Houssin, J. Cramer, R. Grojsman, L. Bellahsene, G.Colas, H. Moulet, W. Minnella, C. Pannetier, M. Leberre, A. Plecis and Y. Chen, Lab Chip , 2016, 16, 1401 – 1411.

62. S. O. Sundberg, C. T. Wittwer, R. M. Howell, J. Huuskonen, R. J. Pryor, J. S. Farrar, H. M. Stiles, R. A. Palais and I. T. Knight,Clin. Chem., 2014, 60, 1306 –1313

63. C. Hurth, J. Yang, M. Barrett, C. Brooks, A. Nordquist, S. Smith and F. Zenhausern,Biomed. Microdevices, 2014, 16, 905 –914.

64. Y. Sun, R. Dhumpa, D. D. Bang, J. Hogberg, K. Handbe rg and A. Wolff, Lab Chip , 2011, 11, 1457 – 1463.

65. S. Jung, J. Kim, D. J. Lee, E. H. Oh, H. Lim, K. P. Kim, N.Choi, T. S. Kim and S. K. Kim, Sci. Rep. , 2016, 6, 22975.

66. K. Qin, X. Lv, Q. Xing, R. Li and Y. Deng, Anal. Method s, 2016, 8, 2584 –2591.

67. S. Ma, D. N. Loufakis, Z. Cao, Y. Chang, L. E. K. Achenie and C. Lu, Lab Chip , 2014, 14, 2905 –2909.

68. C.-Y. Chao, C.-H. Wang, Y.-J. Che, C.-Y. Kao, J.-J. Wu and G.-B. Lee,Biosens. Bioelectron. , 2016, 78, 281–289.

69. P. Liu, X. Li, S. A. Greenspoon, J. R. Scherer and R. A. Mathies, Lab Chip, 2011, 11, 1041 –1048.

70. S.-M. Zhao, L. Zhu, C.-C. Zhu, Y. Li, H.-D. Wang, L. Zhang, D.-W. Du, G.-Q. Deng, A. Wang and Y. Liu, Fenxi Huaxue, 2014, 42, 1393 – 1399.

71. X. Qiu and M. G. Mauk, Microsyst. Technol., 2014, 21, 841 –850.

72. E. A. Oblath, W. H. Henley, J. P. Alarie and J. M. Ramsey, Lab Chip , 2013, 13, 1325 – 1332.

73. D. Cai, M. Xiao, P. Xu, Y. Xu and W. Du, Lab Chip, 2014, 14, 3917 – 3924.

74. D. Le Roux, B. E. Root, C. R. Reedy, J. A. Hickey, O. N. Scott, J. M. Bienvenue, J. P. Landers, L. Chassagn e and P.de Mazancourt, Anal. Chem., 2014, 86, 8192 –8199.

75. D. P. Manage, Y. C. Morrissey, A. J. Stickel, J. Lauzon, A. Atrazhev, J. P. Acker and L. M. Pilarski, Microfluid. Nanofluid., 2010, 10, 697– 702.

76. Y. Liu, C. Li, Z. Li, S. D. Chan, D. Eto, W. Wu, J. P. Zhang, R.-L. Chien, H. G. Wada, M. Greenstein and S. Satomura, Electroph oresis, 2016, 37, 545– 552.

77. S. Furutani, H. Nagai, Y. Takamura and I. Kubo, Anal. Bioanal. Chem., 2010, 398, 2997 –3004.

78. S. Furutani, H. Nagai, Y. Takamura, Y. Aoyama and I. Kubo, Analyst, 2012, 137 , 2951 –2957.

79. M. Amasia , M. Cozzens and M. J. Madou,Sens. Actuators, B , 2012, 161 , 1191 –1197.

80. O. Strohmeier, S. Laßmann, B. Riedel, D. Mark, G. Roth, M. Werner, R. Zengerle and F. Stetten, Microchim. Acta, 2013, 181, 1681 –1688.

81. M. Keller, S. Wadle, N. Paust, L. Dreesen, C. Nuese, O. Strohmeier, R. Zengerle and F. von Stetten, RSC Adv., 2015, 5, 89603– 89611.

82. O. Strohmeier, N. Marquart, D. Mark, G. Roth, R. Zengerle and F. von Stetten, Anal. Methods, 2014, 6, 2038 –2046.

83. M. Keller, J. Naue, R. Zengerle, F. von Stetten and U. Schmidt, PLoS One, 2015, 10, e0131845.

84. G. Czilwik, I. Schwarz, M. Keller, S. Wadle, S. Zehnle, F. von Stetten, D. Mark, R. Zengerle and N. Paust, Lab Chip, 2015, 15, 1084 – 1091.

85. G. Czilwik, T. Messinger, O. Strohmeier, S. Wadle, F. von Stetten, N. Paust, G. Roth, R. Zengerle, P. Saarinen, J. Niittymaki, K. McAllister, O. Sheils, J. O'Leary and D. Mark, Lab Chip , 2015, 15, 3749 –3759.

86. H. Kim, S. Vishniakou and G. W. Faris, Lab Chip, 2009, 9, 1230–1235.

87. Y. Zhu, Y.-X. Zhang, W.-W. Liu, Y. Ma, Q. Fang and B. Yao, Sci. Rep., 2015, 5, 9551.

88. Y. Xu, H. Yan, Y. Zhang, K. Jiang, Y. Lu, Y. Ren, H. Wang, S. Wang and W. Xing, Lab Chip, 2015, 15, 2826–2834.

89. F. Stumpf , J. Schoendube, A. Gross, C. Rath, S. Niekrawietz, P. Koltay and G. Roth, Biosens. Bio electron. 2015, 69, 301 – 306.

90. H. Sun, T. Olsen, J. Zhu, J. Tao, B. Ponnaiya, S. A. Amundson, D. J. Brenner and Q. Lin, RSC Adv., 2015, 5, 4886–4893.

91. S. W. Lim, T. M. Tran and A. R. Abate, PLoS One, 2015, 10, e0113549.

92. V. Sanchez-Freire, A. D. Ebert, T. Kalisky, S. R. Quake and J. C. Wu, Nat. Protoc., 2012, 7, 829– 838.

93. K. H. Narsinh, N. Sun, V. Sanchez-Freire, A. SLee, P. Almeida, S. Hu, T. Jan, K. D. Wilson, D. Leong, J. Rosenberg, M. Yao, R. C. Robbins and J. C. Wu,J. Clin. Invest. , 2011, 121, 1217 –1221.

94. A. K. White, M. VanInsb erghe, O. I. Petriv, M. Hamidi, D. Sikorski, M. A. Marra, J. Piret, S. Aparicio and C. L. Hansen, Proc. Natl. Acad. Sci. U. S. A., 2011, 108 , 13999–14004.

95. M. C. Giuffrida, L. M. Zanoli, R. D'Agata, A. Finotti, R. Gambari and G. Spoto, Anal. Bioanal. Chem., 2015, 407, 1533–1543.

96. T. D. Rane, L. Chen, H. C. Zec and T.-H. Wang, Lab Chip, 2015, 15, 776–782.

97. J. Luo, X. Fang, D. Ye, H. Li, H. Chen, S. Zhang and J. Kong, Biosens. Bioelectron. , 2014, 60, 84 – 91.

98. L. Desbois, A. Padirac, S. Kaneda, A. J. Genot, Y. Rondelez, D. Hober, D. Collard and T. Fujii,Biomicrofluidics , 2012, 6 , 044101.

99. C.-H. Wang, K.-Y. Lien, T.-Y. Wang, T.-Y. Chen and G.-B. Lee, Biosens. Bioelectron. , 2011, 26, 2045 –2052.

100. T. Wang, Y. Zhang, G. Huang, C. Wang, L. Xie, L. Ma, Z. Li, X. Luo, H. Tian, Q. Li, X. Li, Z. Lv and X. Bao, Sci. China: Chem. , 2012, 55, 508–514.

101. Q.-J. Zhou, L. Wang, J. Chen, R.-N. Wang, Y.-H. Shi, C.-H. Li, D.-M. Zhang, X.-J. Yan and Y.-J. Zhang, J. Microbiol. Methods, 2014, 104 ,26 –35.

102. A. A. Sayad, F. Ibrahim, S. M. Uddin, K. X. Pei, M. S. Mohktar, M. Madou and K. L. Thong, Sens. Actuators, B, 2016, 227 , 600–609.

103. Y. Zhang, L. Zhang, J. Sun, Y. Liu, X. Ma, S. Cui, L. Ma, J. J. Xi and X. Jiang, Anal. Chem., 2014, 86, 7057 –7062.

104. C. Liu, M. G. Mauk and H. H. Bau,Microfluid. Nanofluid., 2011, 11, 209–220.

105. K. Hsieh, B. S. Ferguson, M. Eisenstein, K. W. Plaxco and H. T. Soh,Acc. Chem. Res. , 2015, 48, 911–920.

106. X. Fang, H. Chen, S. Yu, X. Jiang and J. Kong, Anal. Chem., 2011, 83, 690–695.

107. P. Zhu, W. Fu, C. Wang, Z. Du, K. Huang, S. Zhu and W. Xu, Anal. Chim. Acta, 2016, 916 ,60 – 66.

108. X. Bian, F. Jing, G. Li, X. Fan, C. Jia, H. Zhou, Q. Jin and J. Zhao, Biosens. Bioelectron. , 2015, 74, 770–777.

109. Q. Zhong, S. Bhattacharya, S. Kotsopoulos, J. Olson, V. Taly, A. D. Griffiths, D. R. Link and J. W. Larson, Lab Chip, 2011, 11, 2167 – 2174.

110. P. Wang, F. Jing, G. Li, Z. Wu, Z. Cheng, J. Zhang, H. Zhang, C. Jia, Q. Jin, H. Mao and J. Zhao, Biosens. Bioelectron ., 2015, 74, 836–842.

111. Y. Men, Y. Fu, Z. Chen, P. A. Sims, W. J. Greenleaf and Y. Huang,Anal. Chem., 2012, 84, 4262 –4266.

112. K. A. Heyries, C. Tropini , M. VanInsb erghe, C. Doolin, O. I. Petriv, A. Singhal, K. Leung, C. B. Hughesman and C. L. Hansen, Nat. Methods , 2011, 8 , 649–651.

113. H. Tanaka, S. Yamamoto, A. Nakamura, Y. Nakashoji, N. Okura, N. Nakamoto, K. Tsukagoshi and M. Hashimoto, Anal. Chem., 2015, 87, 4134 –4143.

114. A. M. Thompson, A. Gansen, A. L. Paguirigan, J. E. Kreutz, J. P. Radich and D. T. Chiu, Anal. Chem., 2014, 86, 12308 – 12314.

115. Q. Song, Y. Gao, Q. Zhu, Q. Tian, B. Yu, B. Song, Y. Xu, M. Yuan, C. Ma, W. Jin, T. Zhang, Y. Mu and Q. Jin, Biomed. Microde vices, 2015, 17, 1–8.

116. Q. Tian, Q. Song, Y. Xu, Q. Zhu, B. Yu, W. Jin, Q. Jin and Y. Mu, Anal. Method s, 2015, 7, 2006 – 2011.

117. X. Leng, W. Zhang, C. Wang, L. Cui and C. J. Yang, Lab Chip, 2010, 10, 2841 –2843.

118. D. Paunescu, C. A. Mora, L. Querci, R. Heckel, M. Puddu, B. Hattendor f, D. Günther and R. N. Grass,ACS Nano, 2015, 9 , 9564–9572.

119. S. O. Sundberg, C. T. Wittwe r, L. Zhou, R. Palais, Z. Dwight and B. K. Gale, Biomed. Microdevices, 2014, 16, 639–644.

120. F. Schuler, F. Schwemmer, M. Trotter, S. Wadle, R. Zengerle, F. von Stetten and N. Paust, Lab Chip, 2015, 15, 2759–2766.

121. F. Schuler, M. Trotter, M. Geltman, F. Schwemm er, S. Wadle, E. Dominguez-Garrido, M. Lopez, C. Cervera-Acedo, P. Santibanez, F. von Stetten, R. Zengerle and N. Paust, Lab Chip, 2016, 16, 208– 216.

122. F. Schuler, C. Siber, S. Hin, S. Wadle, N. Paust, R. Zengerle and F. von Stetten, Anal. Methods, 2016, 8, 2750 –2755.

123. W. Du, L. Li, K. P. Nichols and R. F. Ismagilov, Lab Chip , 2009, 9 , 2286 –2292.

124. B. Sun, F. Shen, S. E. McCalla , J. E. Kreutz, M. A. Karymov and R. F. Ismagilov, Anal. Chem. , 2013, 85, 1540–1546.

125. D. A. Selck, M. A. Karymov, B. Sun and R. F. Ismagilov, Anal. Chem., 2013, 85, 11129–11136.

126. GenePOC, http://www.gene poc-diagnostics.com/en/technology/, (accessed 31.08.2016).

127. Roche Diagnostics, https: //usdiagnostics.roche.com/en/instrument/cobas-liat.html, (accessed 31.08.20 16).

128. BD Diagnostic Systems, http://moleculardiagnostics.bd.com/product/max/, (accessed 31.08.2016).

129. Hunicke-Smith SP, "PCR and cycle sequencing reactions: a new device and engineering model (Ph.D. Thesis)," Stanford University, 1997.

130. Y. Wang, K. Pant, J. Grover, S. Sundaram, "Multiphysics simulational analysis of a novel PCR micro-device," Nanotech, vol. 3, pp. 456–459, 2007.

CERTIFICATE OF COMPLETENESS

It is hereby certified that the dissertation submitted by **NS Mohsin Raza**, Reg No. **00000119573**, Titled: **Thermal Design and Analysis of Static Chamber Microfluidic Device**

has been checked/reviewed and its contents are complete in all respects.

Supervisor's Name: **Dr. Imran Akhtar** Signature: _____

Date: _____